NASA TM X-53571

GPO PRICE $ _____

CFSTI PRICE(S) $ _____

Hard copy (HC) __300____

Microfiche (MF) __.65____

ff 653 July 65

FEASIBILITY STUDIES OF A SHORT DURATION HIGH REYNOLDS NUMBER TUBE WIND TUNNEL

By John W. Davis and Hal S. Gwin
    Aero-Astrodynamics Laboratory

N68-18190

(ACCESSION NUMBER)   (THRU)

56
(PAGES)   (CODE)

TMX-53571
(NASA CR OR TMX OR AD NUMBER)   (CATEGORY)

FACILITY FORM 602

NASA

George C. Marshall
Space Flight Center,
Huntsville, Alabama

TECHNICAL MEMORANDUM X-53571

FEASIBILITY STUDIES OF A SHORT DURATION
HIGH REYNOLDS NUMBER TUBE WIND TUNNEL

By

John W. Davis and Hal S. Gwin

ABSTRACT

A relatively inexpensive short duration test facility is described
in which extremely high Reynolds number flows are practical in the sub-
sonic, transonic, and supersonic speed ranges. Basically, the method
described is a type of blowdown wind tunnel in which the air storage
vessels have been replaced by a long tube filled with high pressure gas.
Upon bursting of a diaphragm, a short duration steady flow is achieved
behind the centered rarefaction fan which propagates into the supply
tube. Useful testing may be accomplished during this period by expand-
ing the gas to the desired test condition by conventional means.

Experimental results are presented indicating primarily the transient
starting characteristics of a small scale pilot model facility tested.
Experimentally determined test data showed close agreement with those pre-
dicted by unsteady expansion theory.

NASA - GEORGE C. MARSHALL SPACE FLIGHT CENTER

NASA - GEORGE C. MARSHALL SPACE FLIGHT CENTER

Technical Memorandum X-53571

January 9, 1968

FEASIBILITY STUDIES OF A SHORT DURATION HIGH REYNOLDS NUMBER TUBE WIND TUNNEL

By

John W. Davis and Hal S. Gwin

GAS DYNAMICS SECTION
EXPERIMENTAL AEROPHYSICS BRANCH
AEROPHYSICS DIVISION
AERO-ASTRODYNAMICS LABORATORY
RESEARCH AND DEVELOPMENT OPERATIONS

PRECEDING PAGE BLANK NOT FILMED.

TABLE OF CONTENTS

LIST OF ILLUSTRATIONS

DEFINITION OF SYMBOLS

Symbol	Definition
A	dimensionless quantity a/a_o
a	acoustic speed
b	cross-sectional area
C_+	foreward facing characteristic
C_-	rearward facing characteristic
D	quantity $1 + \frac{\gamma - 1}{2} M$
ℓ	length of supply tube
M	Mach number
P	pressure
R_e	Reynolds number
T	temperature
t	time
U	dimensionless quantity u/u_o
u	particle velocity
χ	dimensionless quantity x/ℓ
x	position along the supply tube measured from the diaphragm
α	dimensionless quantity $\frac{\gamma + 1}{\gamma - 1}$
β	dimensionless quantity $\frac{\gamma - 1}{2\gamma}$

Symbol	Definition
γ	ratio of specific heats
ρ	density
τ	dimensionless quantity ta_o/ℓ

SUBSCRIPTS

o	initial conditions in supply tube
1	quasi-steady conditions in supply tube behind the incident rarefaction wave
*	critical conditions (i.e., conditions where the local speed is equal to the local speed of sound)
i	point of intersection of the head of the reflected rarefaction wave and the tail of the incident wave
r	time at which the head of the incident wave returns to its position of origin
t	total conditions
t_1	total conditions just upstream of shock wave
t_2	total conditions just downstream of shock wave

FEASIBILITY STUDIES OF A SHORT DURATION
HIGH REYNOLDS NUMBER TUBE WIND TUNNEL

SUMMARY

A relatively inexpensive short duration test facility is described
in which extremely high Reynolds number flows are practical in the sub-
sonic, transonic, and supersonic speed ranges. Basically, the method
described is a type of blowdown wind tunnel in which the air storage
vessels have been replaced by a long tube filled with high pressure gas.
Upon bursting of a diaphragm, a short duration steady flow is achieved
behind the centered rarefaction fan which propagates into the supply
tube. Useful testing may be accomplished during this period by expand-
ing the gas to the desired test condition by conventional means.

Experimental results are presented indicating primarily the trans-
ient starting characteristics of a small scale pilot model facility
tested. Experimentally determined test data showed close agreement with
those predicted by unsteady expansion theory.

I. INTRODUCTION

Designers have long been faced with the solution of a number of
Reynolds number dependent aerodynamic and thermodynamic problems in the
design and testing of large boost vehicles. In many cases it has been
permissible to violate the Reynolds similarity law when suitable test
facilities do not exist. However, some aerodynamic problems, such as
loads distribution at high angles of attack, shock-induced boundary
layer separation, aerodynamic noise, and certain aspects of base heat-
ing, seem to exhibit Reynolds number effects of an unknown character
and magnitude, even with a turbulent boundary layer [1]. To obtain data
in these areas, MSFC proposed in 1964 the construction of a relatively
inexpensive short duration blowdown wind tunnel, based on the Ludwieg tube
wind tunnel concept, which would be capable of simulating full scale
Saturn V trajectory Reynolds numbers, of the order of 1×10^9 based on
vehicle length, over a Mach number range from 0.2 to 4.0 for test periods
of approximately 0.5 seconds.

Figure 1 shows the Reynolds number simulation requirements of several current launch vehicles, proposed future launch vehicles, and supersonic aircraft. This figure shows that Reynolds number simulation is adequate at Mach numbers above 4.0, and that the prime Reynolds number deficiency exists in the transonic and low supersonic speed ranges where many aerodynamic problems are most pronounced.

With these factors in mind, analytical and experimental studies have been conducted on a number of the engineering problems involved in such a facility with emphasis in the transonic area. A small pilot model has been constructed to verify experimentally the feasibility of such a facility, to check the principle of operation, and to assess its usefulness. Results of these studies are presented, along with a description of the principles of operation of such a facility.

II. FACILITY CONCEPT

The tube wind tunnel was suggested in 1955 by Ludwieg [2]. This type of facility is essentially a simplified blowdown wind tunnel with the storage vessel or vessels replaced by a long supply tube. Similar principles have been applied by Cornell Aeronautical Laboratory to simulate certain base heating conditions under MSFC Contract NAS8-823.

The basic concept of the tube wind tunnel is shown in Figure 2 where the diaphragm is located upstream of the nozzle. When the diaphragm is broken, a backward-facing centered rarefaction fan propagates into the supply tube, setting the gas in motion and lowering the pressure and temperature somewhat. The rarefaction fan travels along the supply tube, is reflected off the closed end, and returns to the nozzle throat where it is again reflected and the wave process repeated for several cycles. Also, subsequent to the rupturing of the diaphragm, a shock wave and contact surface proceed downstream. Between the time when the nozzle-starting process has ended and when the head of the reflected rarefaction wave arrives at the nozzle throat, useful testing can be accomplished in the test section under constant reservoir conditions. Subsequent test periods may be obtained at reduced reservoir conditions between re-reflected wave processes. Normally, the test gas would be discharged to the atmosphere after passing through the test section.

In the concept actually advanced by Ludwieg, the diaphragm was employed downstream of the test section. The wave process for such a case is somewhat different, reflecting a more complicated starting process. For this case rarefaction waves may pass through the nozzle into the supply tube only until sonic velocity is reached at the throat. At this point, a normal shock wave forms and gradually moves to the nozzle exit. The remainder of the rarefaction fan weakens the shock, and it is eventually swept through the test section, commencing the period of steady flow..

2

Location of the diaphragm at either of the previously mentioned stations has its own merits. The physical size, complexity, and cost would be less for a diaphragm located downstream of the test section than for a diaphragm located in the larger diameter supply tube. For an upstream diaphragm location the starting shock and contact surface generated upon bursting of the diaphragm pass over the test article and can produce a starting impulse. This problem is avoided with a downstream diaphragm since the disturbance does not pass through the test section. However, the upstream diaphragm location allows a considerably faster tunnel start time, and permits the possible reduction of model starting loads by the initial evacuation of the test section. The possibility of diaphragm particles striking the test article must be considered with the upstream location, whereas severe instrumentation problems arise in measuring static pressures in the supersonic speed range when a downstream diaphragm is used.

III. THEORY OF OPERATION

The wave diagram shown in Figure 2 indicates the incident centered rarefaction fan propagated in the supply tube after instantaneous bursting of the diaphragm and its path after being reflected off the closed end of the supply tube. It will be assumed that the flow in the constant diameter supply tube is one-dimensional, the test medium is a perfect gas, and the flow ahead of the nozzle entrance is subsonic.

For an isentropic flow the velocity of a rearward-facing wave (C_-) in the (x,t) plane is given by

$$\frac{dx}{dt} = u - a. \tag{1}$$

Along any characteristic,

$$\frac{2a}{\gamma - 1} - u = \text{constant}, \tag{2}$$

and, across the entire wave,

$$\frac{2a}{\gamma - 1} + u = \text{constant}. \tag{3}$$

Similarly, for a forward-facing wave (C_+), the velocity is given by

$$\frac{dx}{dt} = u + a. \tag{4}$$

Along any characteristic

$$\frac{2a}{\gamma - 1} + u = \text{constant}, \tag{5}$$

and, across the entire wave,

$$\frac{2a}{\gamma - 1} - u = \text{constant}. \tag{6}$$

Equations (1) through (6) are fundamental relations for simple wave motion derived from Euler's momentum equation and from the equation of continuity in many references [e.g., 3,4].

Then for a centered rarefaction wave moving to the left, the C_- characteristics are straight lines radiating from the origin with a characteristic slope:

$$\frac{x}{t} = u - a. \tag{7}$$

In region (0) the gas is at rest ($U_0 = 0$), and from equation (7), the velocity of the head of the incident wave becomes

$$\frac{x}{t} = -a_0.$$

When the head of the rarefaction wave reaches the closed end of the supply tube, it is reflected as a rarefaction wave. In the region where the reflected wave passes through the incident wave, the process is one of two equal rarefactions traveling in opposite directions interacting with each other. In this region the path is nonlinear and for the C_+ characteristics,

$$\frac{dx}{dt} = u + a. \tag{8}$$

4

The path in the (X, τ) plane of the head of the incident rarefaction wave after reflection from the end of the supply tube is given by

$$X = (\alpha - 1) \tau - \alpha \tau^{1 - \frac{2}{\alpha}}. \tag{9}$$

Equation (9) has been developed in the appendix. The solution applies only between the head and the tail of the incident rarefaction wave. This is sufficient, however, since the remaining path to the right for the C_+ characteristic is linear as given by the relation

$$\frac{x}{t} = u + a. \tag{10}$$

The position in the (X, τ) plane where the head of the reflected rarefaction wave reaches the tail of the incident wave is given by

$$X_i = \left[\alpha - 1 - \alpha (P_1/P_0)^\beta \right] (P_1/P_0)^{-\beta\alpha/2} \tag{11}$$

and

$$\tau_i = (P_1/P_0)^{-\beta\alpha/2}. \tag{12}$$

The derivation of equations (11) and (12) may also be found in the appendix.

Using equations (10), (11), and (12), we find the relation for the time required for the head of the incident wave to travel to the closed end of the supply tube, reflect, and return to its originating position (τ_r). This is the period of time when constant stagnation conditions exist at the entrance to the nozzle if the diaphragm is located at the nozzle entrance, and is given by

$$\tau_r = \frac{2}{1 + M_1} \left[1 + \frac{\gamma - 1}{2} M_1 \right]^{\frac{\gamma + 1}{2(\gamma - 1)}}. \tag{13}$$

Equation (13) is also derived in the appendix.

To obtain the conditions in region (1), we may, for a rearward-facing wave, use equation (3) to obtain conditions across the entire wave such that

$$\frac{2a_1}{\gamma - 1} + u_1 = \frac{2a_0}{\gamma - 1} + u_0, \tag{14}$$

and since the gas is at rest in region (0) equation (14) becomes

$$\frac{2a_1}{\gamma - 1} + u_1 = \frac{2a_0}{\gamma - 1} . \tag{15}$$

The variation of the velocity of sound with the supply tube Mach number may be found by rearranging equation (15) and substituting $M_1 = u_1/a_1$ such that

$$\frac{u_1}{a_1} + \frac{2}{\gamma - 1} = \frac{2a_0}{a_1(\gamma - 1)} , \tag{16}$$

which results in

$$\frac{a_1}{a_0} = \frac{1}{1 + \frac{\gamma - 1}{2} M_1} . \tag{17}$$

Similarly, the variation of the gas velocity u with the supply tube Mach number may be found using equations (15) and (17)

$$\frac{u_1}{a_0} = \frac{M_1}{1 + \frac{\gamma - 1}{2} M_1} . \tag{18}$$

Under the assumptions of isentropic flow of a perfect gas, other parameters of state related to the velocity of sound may be obtained:

$$\frac{a_1}{a_0} = \sqrt{T_1/T_0} = (P_1/P_0)^{\frac{\gamma-1}{2\gamma}} = (\rho_1/\rho_0)^{\frac{\gamma-1}{2}} . \tag{19}$$

6

It follows that the relationship between the pressure ratio across the rarefaction fan and the supply tube Mach number is given by

$$\frac{P_1}{P_o} = \left(1 + \frac{\gamma - 1}{2} M_1\right)^{-\frac{2\gamma}{\gamma - 1}} . \tag{20}$$

Similarly, the temperature ratio becomes

$$\frac{T_1}{T_o} = \left(1 + \frac{\gamma - 1}{2} M_1\right)^{-2} . \tag{21}$$

The stagnation conditions at the entrance to the nozzle are those which would result from bringing the flow behind the incident unsteady rarefaction to rest. Then using equations (20) and (21), it may be shown that

$$\frac{P_t}{P_o} = \frac{\left(1 + \frac{\gamma - 1}{2} M_1^2\right)^{\frac{\gamma}{\gamma - 1}}}{\left(1 + \frac{\gamma - 1}{2} M_1\right)^{\frac{2\gamma}{\gamma - 1}}} . \tag{22}$$

$$\frac{T_t}{T_o} = \frac{1 + \frac{\gamma - 1}{2} M_1^2}{\left(1 + \frac{\gamma - 1}{2} M_1\right)^{2}} . \tag{23}$$

Thus, we see from equations (13), (20), and (21) that the period of steady flow conditions in the supply tube and the magnitude of the pressure and temperature at the entrance of the nozzle are dependent only on the ratio of specific heats of the test gas, the initial conditions in the supply tube, and the supply tube Mach number. Further, the supply

tube Mach number is a function of the ratio of the supply tube area to the nozzle throat area, defined in reference 5 as

$$\frac{b}{b_*} = \frac{1}{M_1} \left[\frac{1 + \frac{\gamma - 1}{2} M_1^2}{\frac{\gamma + 1}{2}} \right]^{\frac{\gamma+1}{2(\gamma-1)}} . \tag{24}$$

The relationship of the stagnation conditions with respect to the initial supply tube conditions is shown in figure 3 as a function of supply tube Mach number for $\gamma = 1.4$. The rate of recovery with respect to the initial conditions decreases steadily with increasing supply tube Mach number. The duration of steady flow at the nozzle entrance is shown in nondimensional form in figure 4 as a function of supply tube Mach number. Again, the effect is a steadily decreasing test period as the supply tube Mach number increases.

This analysis neglects any effects of the incident shock wave and interface generated upon bursting of the diaphragm. These effects are considered small. Starting characteristics of the nozzle and test section for an upstream diaphragm location are similar to other wind tunnel facilities and are not treated herein. A discussion of this subject may be found in reference 6 or reference 7, for example.

8

IV. DESCRIPTION OF PILOT MODEL FACILITY

Schematic drawings indicating all major components and several component configurations of the pilot model facility are shown in figure 5. Major components included the supply tube, a sonic nozzle, supersonic 7-degree-included-angle conical nozzles for Mach numbers 1.7 and 3.5, a supersonic and transonic test section of 2.61-inch diameter, model and pressure probe support unit, and a diffuser for controlling subsonic Mach numbers. Flow was initiated by cutting multilayer mylar diaphragms supported on a cruciform frame with an air-operated punch housed within the cruciform. Separate diaphragms could be mounted either upstream of the nozzle or downstream of the test section depending on the test requirement. When desired, a settling chamber was installed at the nozzle entrance. The supply tube length could be varied by using alternate combinations of the three tube lengths shown, depending on run-time requirements.

The porous wall configurations of the transonic test section used either 0.125-inch or 0.250-inch diameter holes with a fixed porosity of 22 percent. All holes were inclined 90 degrees to the test section flow. Three plenum chamber volumes were tested using 0.200- to 1.300-inch diameter metering orifices in the four discharge lines to control plenum flow and hence the free stream Mach number. When using a downstream diaphragm configuration, plenum flow was initiated by a separate diaphragm cutter synchronized with the primary diaphragm mechanism.

Tests were conducted at initial supply tube pressures from 250 to 1000 psig allowing investigation of Reynolds number effects on the flow processes. Nitrogen was used as the test medium.

The pilot model facility was installed in the test cell of the MSFC Impulse Base Flow Facility allowing discharge into a large vacuum tank. This permitted operation at different Reynolds numbers with a constant pressure ratio and provided a convenient muffling chamber.

V. EXPERIMENTAL PROGRAM

In an effort to investigate a number of technical problems associated with a facility of this type, a pilot study was conducted with the following objectives:

    (a)   Determination of start time for transonic as well as subsonic and supersonic Mach numbers.

(b) Comparison of performance with theoretical predictions.

(c) Investigation of Reynolds number effects on flow processes.

(d) Comparison of starting times for upstream and downstream diaphragm locations.

(e) Assessment of the effect of supply tube to nozzle throat area contraction ratios on performance.

(f) Investigation of the effect of porous wall hole size on the transonic starting process at constant porosity.

(g) Investigation of starting loads associated with upstream and downstream diaphragm locations.

(h) Assessment of the effect of a settling chamber located ahead of the nozzle increasing the contraction ratio at this point.

Supply tube conditions were evaluated by measuring the static pressure at two positions along the tube as a function of time. Stagnation pressure was derived by knowledge of the theoretical supply tube Mach number and the static pressure measured at a point near the nozzle entrance by means of the following relation [5]:

$$\frac{P}{P_t} = 1 + \frac{\gamma - 1}{2} M^2, \tag{25}$$

where the supply tube Mach number is obtained from equation (24).

For subsonic tests, static pressures were measured with a probe located on the test section centerline. Equation (25) was used to evaluate the test section Mach number once the stagnation pressure had been computed. In a similar manner, the test section Mach number was obtained for supersonic tests from centerline pitot probe measurements from the following relation [5]:

$$\frac{P_{t_2}}{P_{t_1}} = (\gamma + 1)^{\frac{\gamma+1}{\gamma-1}} [2\gamma M^2 - \gamma + 1]^{\frac{1}{1-\gamma}} \left[\frac{(\gamma - 1) M^2 + 2}{M^2} \right]^{\frac{\gamma}{1-\gamma}}. \tag{26}$$

10

Test section Mach number was determined for transonic tests directly from centerline pitot-static probe measurements using the following relation [5]:

$$\frac{P}{P_{t_2}} = 2^{\frac{\gamma}{\gamma-1}} (\gamma + 1)^{\frac{\gamma+1}{1-\gamma}} M^{\frac{2\gamma}{1-\gamma}} [2\gamma M^2 - \gamma + 1]^{\frac{1}{\gamma-1}} . \tag{27}$$

Starting times were defined by measuring the time when the various pressures first responded to the starting process until the test section Mach number and flow properties became completely invariant with respect to time. Only very small changes occurred in the test section flow during the last 25 percent or so of the measured starting period.

During subsonic and supersonic tests, two static pressures were measured along the test section walls as a secondary means of determining the flow properties. Four static pressures were measured at points within the plenum chamber during transonic testing to study the time dependency of the starting process with respect to the adjustment of plenum flow.

All pressures were measured with high response pressure transducers and the data recorded on an F.M. tape system. At the conclusion of each run, the data were read out on a direct writing oscillograph allowing comparison at a common time base.

An attempt was made to determine an approximate relationship between starting and running loads for a cone cylinder frustum type model similar to Saturn type space vehicles. The small 0.261-inch diameter, 2.448-inch length model was mounted on a one-component strain gage balance capable of measuring bending moment in the pitch plane. A view of this model is shown in figure 6. The ratio of the maximum bending moment occurring during the starting process to that existing during the period of steady flow was measured at an angle of attack of 10 degrees. In general, the measurements were subject to large dynamic effects, and being without inertial compensation, they were not suitable for reasonable quantitative results. However, through judicious fairing and averaging of the vibrational envelopes, some qualitative results could be obtained.

VI. RESULTS AND DISCUSSION

Tests were conducted using diaphragms located either upstream of the nozzle or downstream of the test section. During transonic tests, three different plenum volumes were employed, and a series of tests were conducted with a single plenum volume in which two different porous wall hole sizes were used. Also, for certain runs a settling chamber was installed upstream of the nozzle. Subsonic and supersonic configurations were also tested. Data were obtained for each configuration at 250, 500, 750, and 1000 psig initial supply tube pressure.

The general comment can be made that all Reynolds number effects on the test data were negligible, as might well be expected. Accordingly, the data presented are the average of the values obtained at the various Reynolds numbers. An envelope of test Reynolds numbers is shown in figure 7.

Figure 8 compares the starting characteristics of the upstream and downstream diaphragm locations for each 0.250-inch-diameter perforated-wall transonic test section configuration studied. The subsonic region shown is of academic interest in that subsonic flows would normally be generated by choking downstream of the test section. This region reflects the process of removing the test section boundary layer. Thus, further discussion will be directed toward the transonic region. A longer starting process is indicated for a downstream diaphragm location. For plenum volume 1, the starting process for the downstream diaphragm location required approximately 25 percent more time at Mach number 1.0 than the upstream location; while at Mach number 1.2 the deviation has increased to approximately 120 percent. With a downstream diaphragm, the plenum chamber and the supply tube are initially at the same pressure. As the free stream Mach number is increased (by increasing the orifice diameter), the required mass flow through the porous wall increases, and the free stream static pressure decreases, requiring a larger change in the plenum pressure level from the initial value. As shown in figure 8, these requirements result in a steadily increasing start time for a downstream diaphragm location, as the free stream Mach number is increased, the free stream static pressure more nearly approaches the initial plenum chamber value, which may be atmospheric or perhaps below. Although the required porous-wall mass flow for a given Mach number is identical to the downstream case, figure 8 indicates the test section flow and hence the plenum flow adjusts more quickly. Similar results are indicated for each plenum volume configuration tested. Transonic Mach numbers as high as 1.32 were produced for these configurations after starting periods of 50 milliseconds or less.

12

It is apparent in figure 8 and subsequent figures that, in the vicinity of Mach number 1.3, choking of the perforated walls occurs, thus restricting further increase in flow through the wall. The result is that, once choked flow is established, no further increase in test section Mach number is possible, and further increase in the size of the metering orifices in the plenum exhaust only permits the plenum flow to adjust more rapidly; consequently, the start time decreases accordingly.

A cross plot indicating the transonic starting characteristics as a function of plenum volume is shown in figure 9. In general, the starting characteristics when using a diaphragm located upstream of the nozzle varied somewhat linearly with plenum volumes, and for a given plenum volume less start time was required as the Mach number increased. When using a downstream diaphragm, the effect of plenum volume is more significant, particularly at the lower volumes, which obviously produce higher plenum velocities. In this case much more benefit can be derived by maintaining the plenum volume at the absolute minimum consistent with reasonable test section flow. Also, in the downstream diaphragm case, at a given plenum volume, more start time was required as the Mach number increased.

The effect on starting characteristics of different test section porous wall hole sizes is shown in figure 10 for holes of 0.125-inch and 0.250-inch diameter and a porosity of 22 percent. All holes were perpendicular to the test section flow. As would be expected, the smaller holes produced longer starting transients. However, for reasons not presently understood, the test section walls with the smaller holes remained unchoked up to the limit of flow through the plenum exhaust for both the upstream and downstream diaphragm cases, even though test section walls with holes of 0.250-inch diameters choked at a Mach number of approximately 0.15 less than was achieved by unchoked walls with the smaller holes.

Results of tests in the subsonic and supersonic configurations are shown in figure 11. In each case, data are available for only two Mach numbers, and the indicated start-time change with Mach number is perhaps less than the accuracy of measurement. It would be expected that each of these cases would start in less time than the transonic test section at an equivalent Mach number. This result appears true when compared with the supersonic test section data. However, the indications are that the starting transient for the subsonic test section at Mach number 0.7 is greater than that obtained in the transonic test section at approximately the same Mach number.

Adding a settling chamber of proper contraction ratio to provide good test section flow allows a reduction in supply tube size and a correspondingly lower cost for such a facility. Figure 12 shows the effect on start time characteristics of a settling chamber installed

upstream of the nozzle. Apparently, the flow required to fill the settling chamber when using an upstream diaphragm predominates the process and the start time is increased by approximately 2 to 4 times that required without a settling chamber. At the downstream diaphragm location, the settling chamber is initially charged to the same pressure as the supply tube, and only a small pressure adjustment is required after passage of the expansion fan. As shown in figure 12, the change in start time for the downstream diaphragm configuration tested with settling chamber was undetectable when compared to data obtained without the settling chamber.

To allow a more general comparison, the start time data from each test section are summarized in figure 13. For this comparison plenum 1 has been used for transonic data, and all data presented is for the case without a settling chamber.

Theoretical and experimental recovery pressures in the supply tube are compared in figure 14. Agreement between the two is considered good. Lower contraction ratios of the supply tube to the sonic throat produce increasing supply tube Mach numbers and decreasing recovery pressures. Figure 15 shows the relationship between the theoretical steady flow time available in the supply tube and the experimentally determined steady flow time. Since no temperature measurements were obtained, the initial speed of sound of the supply tube gas was deduced from the velocity of the head of the incident rarefaction wave using equation (7) and the condition $u_o = 0$. In many cases the experimental data were obtained at small but significant distances from the diaphragm cutter, and the data were correlated using equations (7) and (10) to include the time of passage over this distance by the head of the incident rarefaction wave and by the head of the reflected rarefaction. The experimental data show reasonably good agreement with one-dimensional theory. As was the case with supply recovery pressures, the time of steady flow in the supply tube decreased with increasing supply tube Mach number, but to a lesser degree.

Because of the small size of the test hardware, the precise measurement of model starting loads was considered impractical. However, it seemed that an assessment of starting load trends could be obtained by measuring the relationship of the bending moment existing in a flexure located immediately behind a typical model during the starting process to the bending moment existing during the period of steady flow. A model typical of Saturn type vehicles was tested, and the data were obtained without the benefit of inertial compensation. In general, the data were subject to high dynamics, and judicious fairing and averaging of the vibrational envelopes were required to obtain the results shown in figure 16. Because of their qualitative nature, these data are presented as two bands, one for the upstream diaphragm and the other for the downstream diaphragm. In each case the lower limit of the band was obtained at an initial supply tube pressure of 65 psia, the upper limit

14

at a pressure of 265 psia, which was the maximum used for investigation of starting loads, and starting loads increased with pressure. In general, the downstream diaphragm data band behaves much like a conventional blow-down wind tunnel with a level steadily increasing with Mach number. With an upstream diaphragm location, apparently the initial disturbance of the shock wave and the ensuing interface propagated upon bursting of the diaphragm significantly influences the unsteady model loads. In this case, the data band is at a maximum in the subsonic range and falls continually with Mach number. The initial evacuation of the test section somewhat lowered the starting loads for the upstream diaphragm case.

VII. CONCLUSIONS

The results of this study indicate the feasibility of producing short duration transonic flows by means of the tube wind tunnel concept. Starting times ranged from 10 to 50 milliseconds for Mach numbers to as high as 1.43. Because of the small size of the test hardware, no measure of shock cancellation properties could be obtained. However, it is envisioned that future tests with larger test section size will indicate the degree of shock cancellation. The feasibility of subsonic and super-sonic testing in such a facility is also indicated.

Further study is required in the optimization of the perforated wall configuration.

The modification of Ludwieg's concept to an upstream diaphragm, with a corresponding simplification of the wave process, results in starting times as much as 55 percent lower than with the downstream dia-phragm. Also the transonic start time with an upstream diaphragm appears less sensitive to increases in plenum volume, and would, for equivalent start times, allow lower plenum velocities and perhaps better test sec-tion flow properties. However, this modification appears to result in a starting load penalty in the subsonic and transonic Mach number ranges.

The use of a settling chamber ahead of the nozzle had a negligible effect on start times when used with a downstream diaphragm, but when used with an upstream diaphragm, approximately 2 to 4 times more start time was required.

Unsteady expansion theory and experimental measurements show good agreement over the range of contraction ratios studied. Reynolds number effects on the various flow processes were negligible for supply tube pressures from 250 to 1000 psia.

While the problem of analyzing the unsteady nozzle and test section starting process is a difficult one, particularly in the case of transonic flows, such a study would be of great value in optimizing this type of short duration facility. It is hoped that such a study can be made in the near future. Such analysis should investigate the practicability of a free jet test section. If suitable, such a test section would allow optical flow visualization techniques in a three-dimensional flow field without producing reflected disturbances from the window wells.

Although this investigation was not intended to be a detailed parametric study of the various problems involved with such a facility and much work remains to be done, the basic concept of producing short duration transonic flows, as well as subsonic and supersonic flows, in a tube wind tunnel appears to have considerable merit.
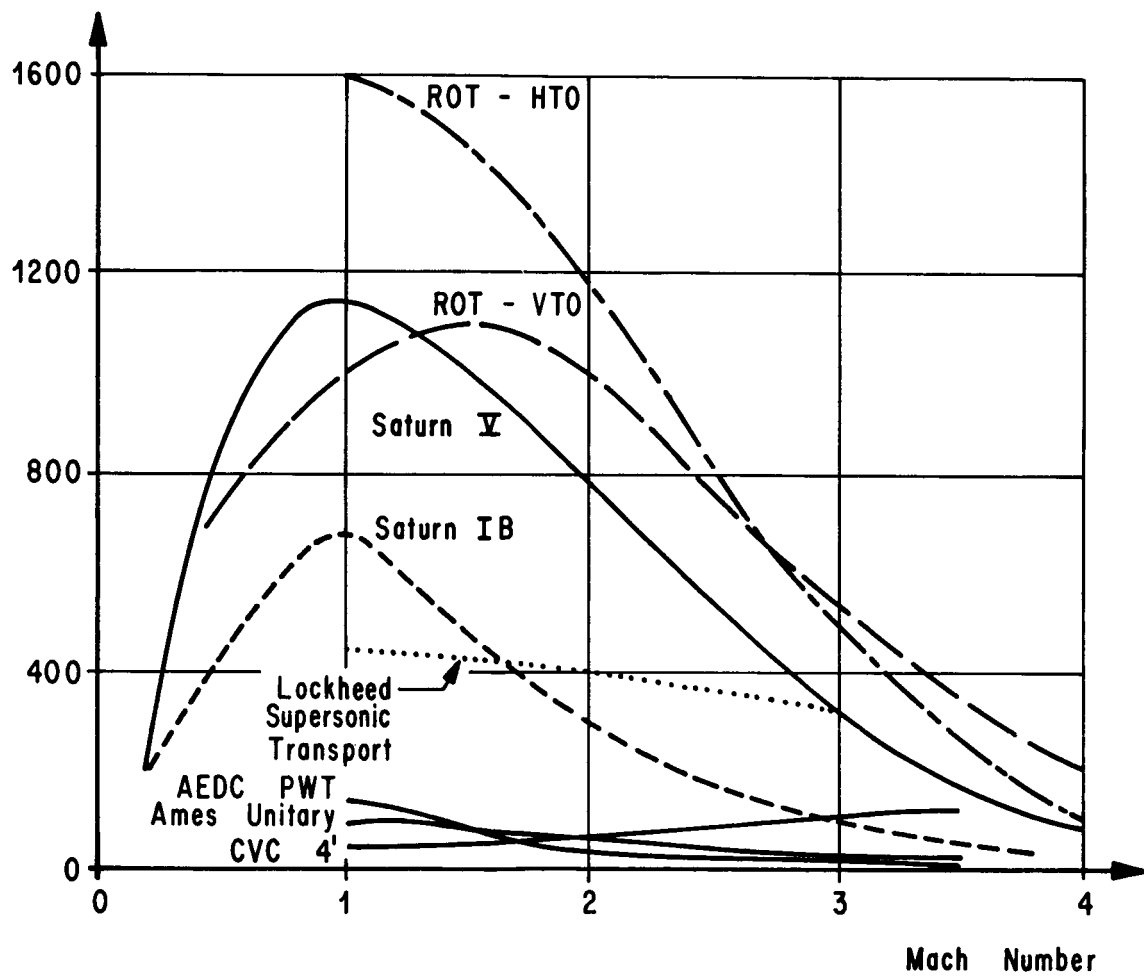
FIG. 1. REYNOLDS NUMBER SIMULATION REQUIREMENTS
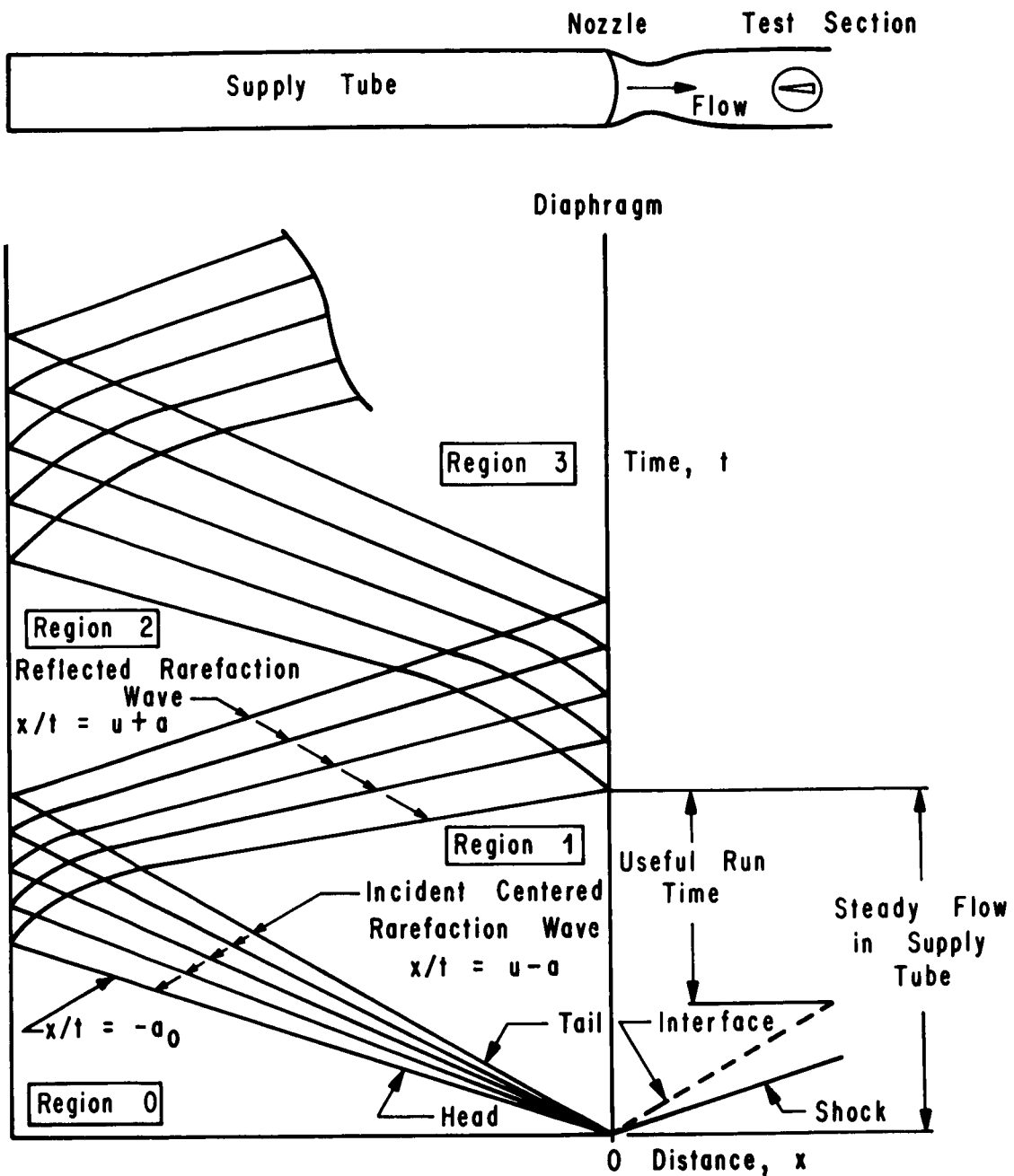
FIG. 2. WAVE DIAGRAM INDICATING
BASIC FACILITY CONCEPT

18
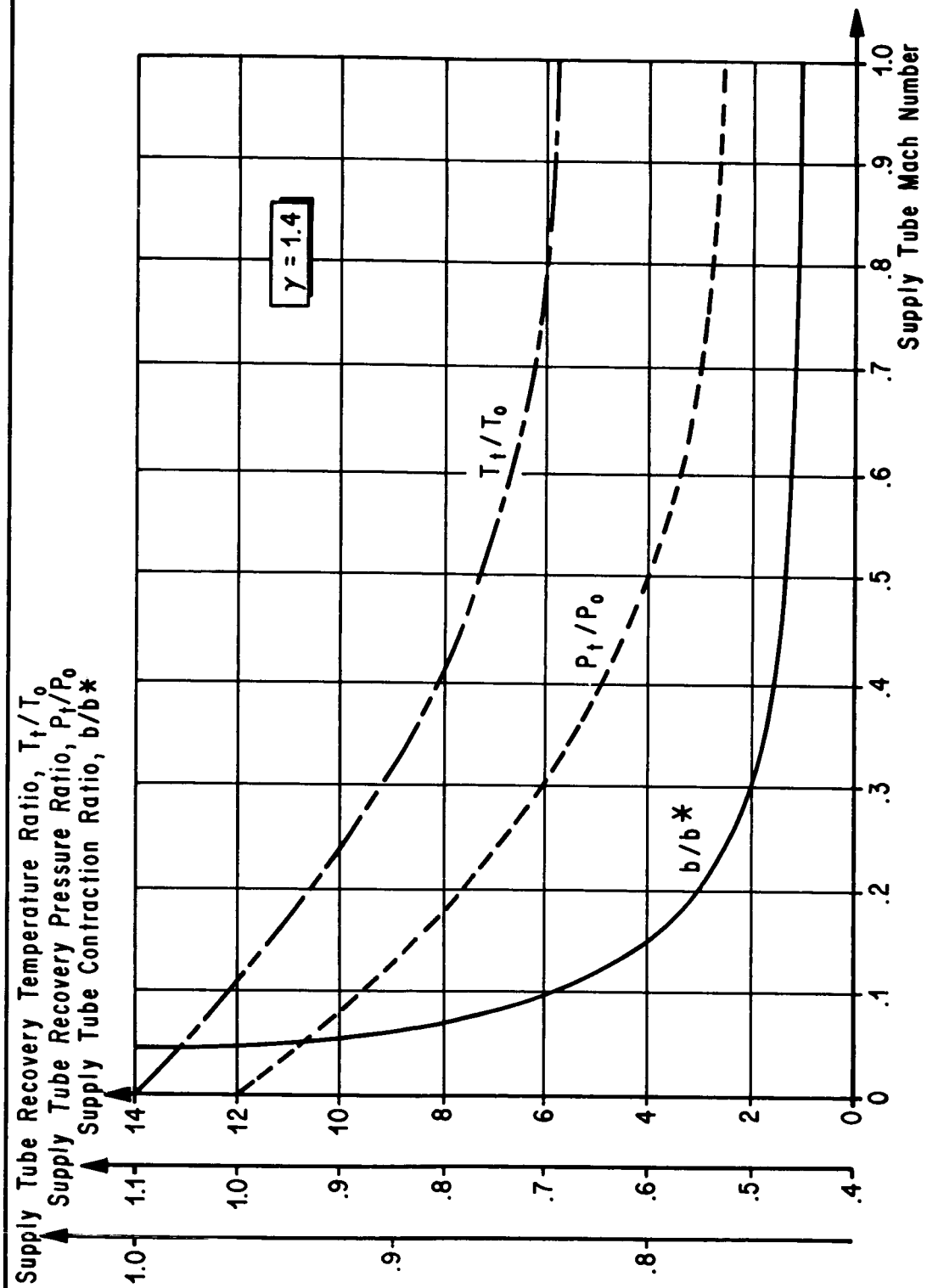
FIG. 3. THEORETICAL VARIATION OF FLOW FIELD PARAMETERS WITH SUPPLY TUBE MACH NUMBER
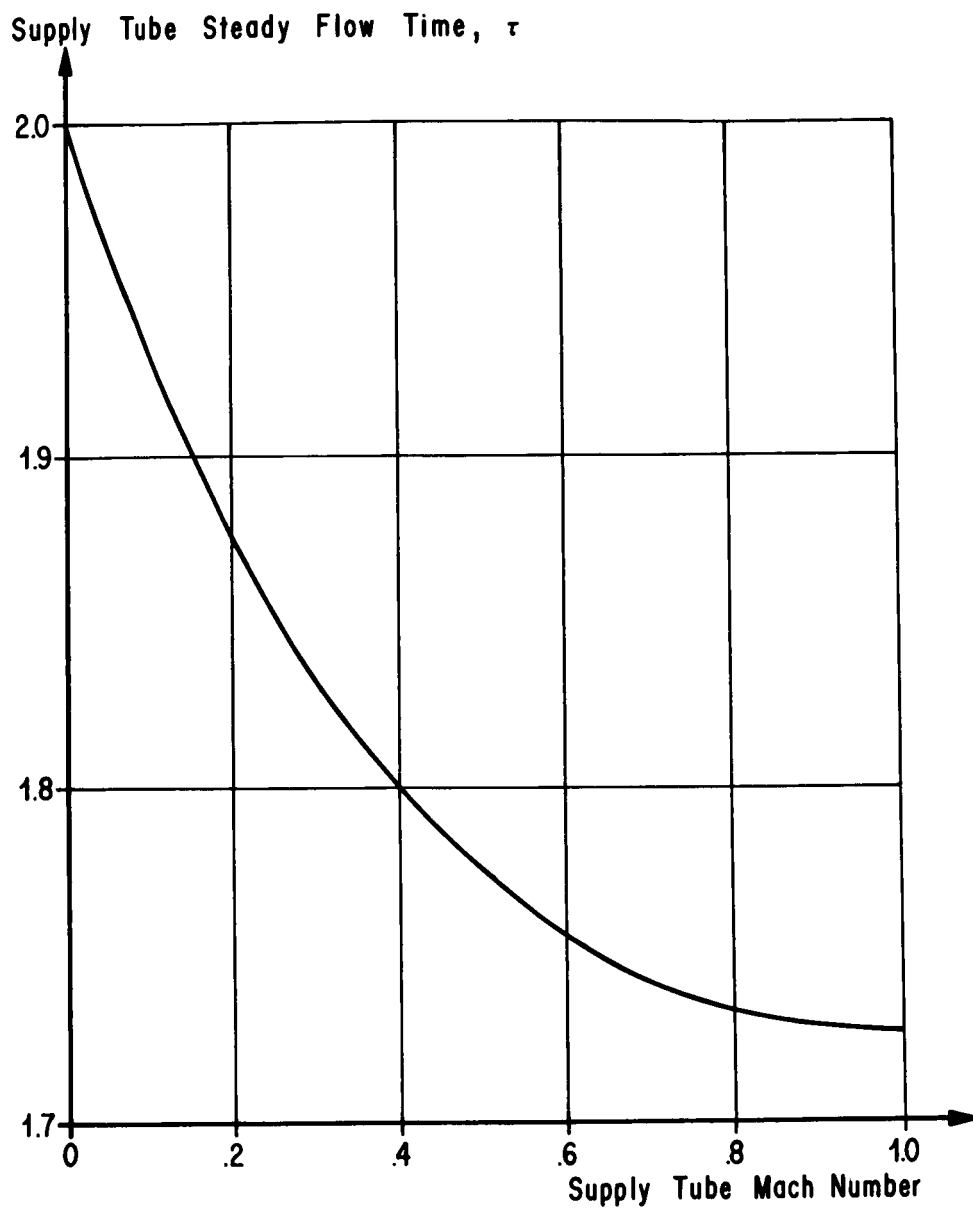
FIG. 4. STEADY FLOW TIME AT NOZZLE ENTRANCE
IN RELATION TO SUPPLY TUBE MACH NUMBER, $\gamma = 1.4$

Supply Tube
(not Shown)
D = 5.76"
L = 440.0"

Supersonic Nozzle
D* = 1.0
L = 15.0

Model Support
D = 2.9
L = 5.25

Diaphragm Cutter
D = 4.0
L = 6.2

Muffler

Vacuum
Tank

Model

Diaphragm

Transition
$D_1 = 4.0$
$D_2 = 2.9$
L = 6.0

Transition
$D_1 = 2.9$
$D_2 = 4.0$
L = 6.0

Test Section
D = 2.61
L = 10.5

Settling Chamber
$D_1 = 5.76"$
$D_2 = 8.25"$
L = 23.50"
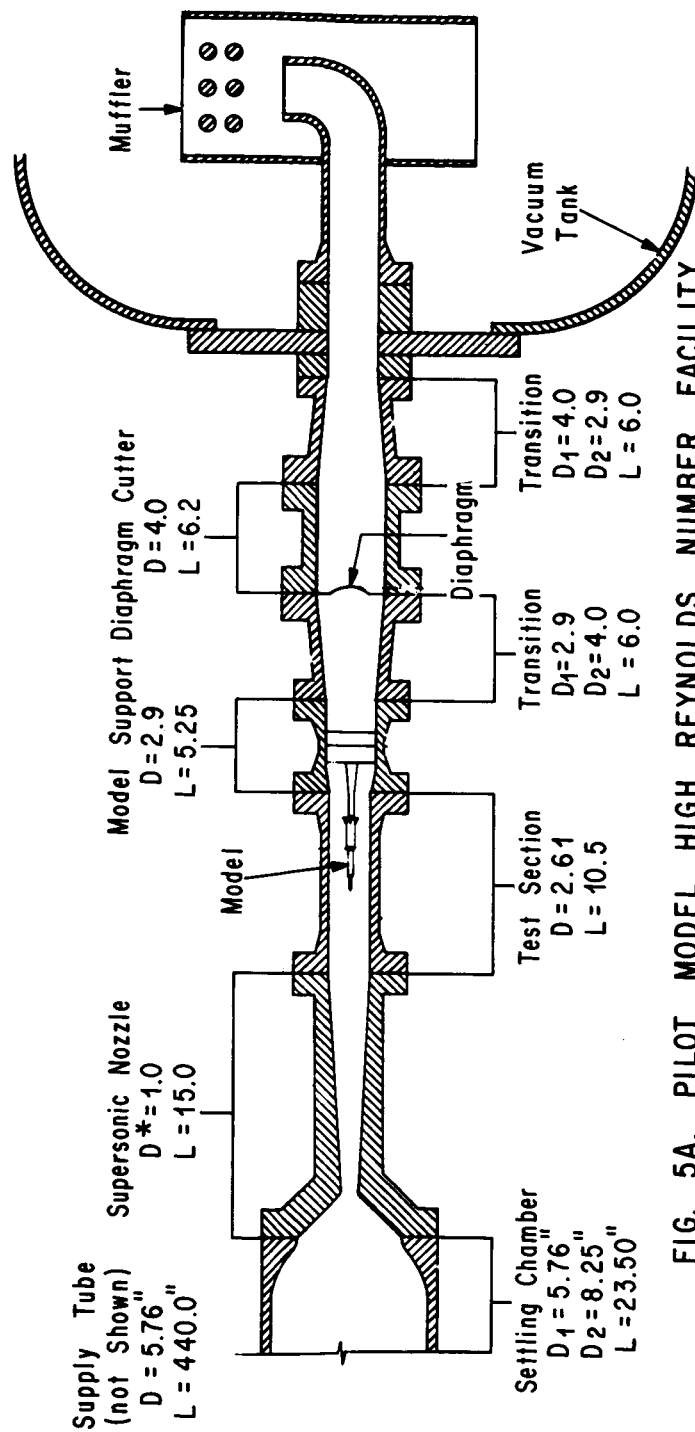
FIG. 5A. PILOT MODEL HIGH REYNOLDS NUMBER FACILITY
SUPERSONIC TEST SECTION CONFIGURATION
DOWNSTREAM DIAPHRAGM POSITION
SETTLING CHAMBER INSTALLED
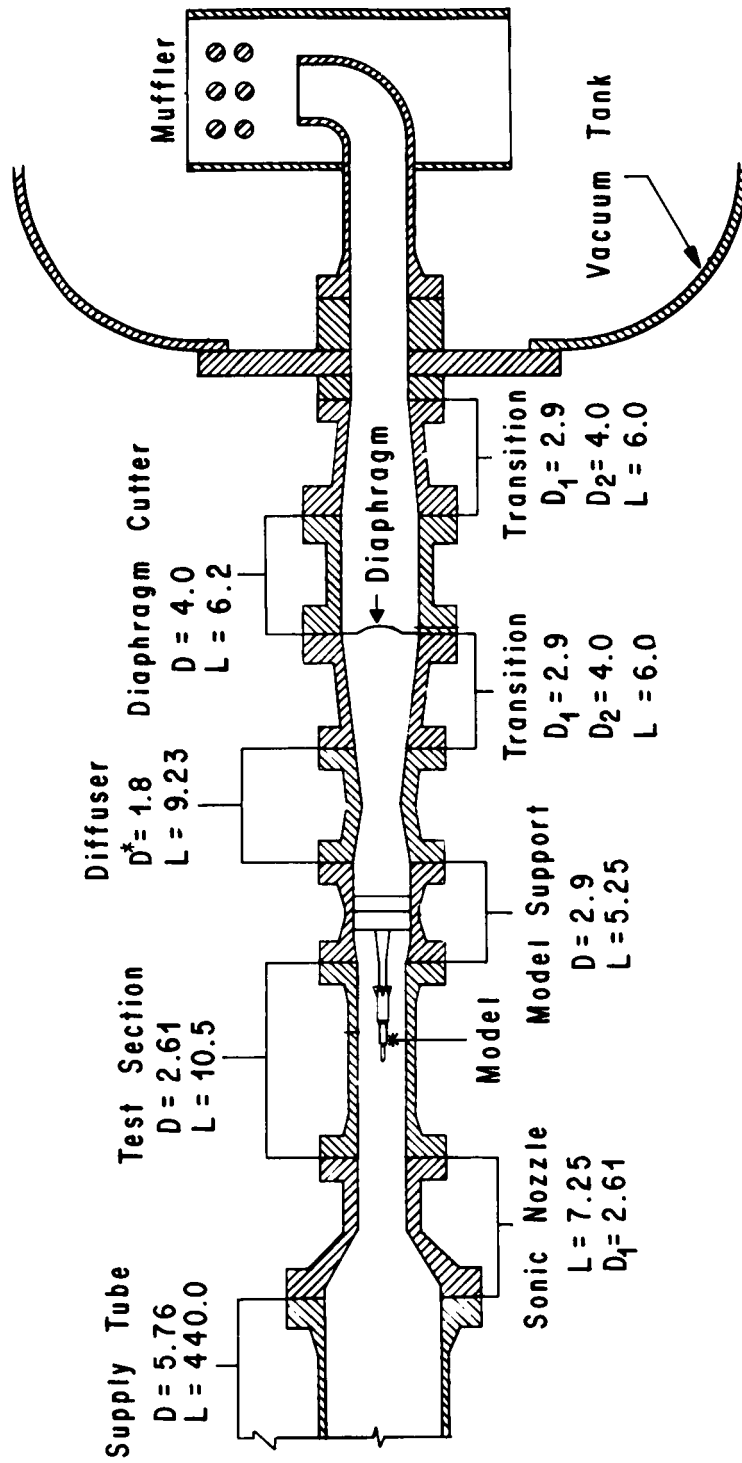
FIG. 5B. PILOT MODEL HIGH REYNOLDS NUMBER FACILITY SUBSONIC TEST SECTION CONFIGURATION DOWNSTREAM DIAPHRAGM POSITION

Plenum Chamber Volume

1 – 20.7 cu.in.
2 – 45.3 cu.in.
3 – 104.5 cu.in.

Model Support
D = 2.9
L = 5.25

Plenum Suction
Line
D = 1.5
L = 96.0

Muffler

Vacuum Tank

Spacer
D = 2.9
L = 8.0

Sonic Nozzle
D = 2.61
L = 7.25

Model

Test Section
D = 2.61
L = 10.5

Interchangable
Plenum Bleed
Orifice

22% Open
Area Porosity
Walls

Supply Tube
D = 5.76
L = 440.0

Diaphragm

Diaphragm Cutter
D = 5.76
L = 7.50
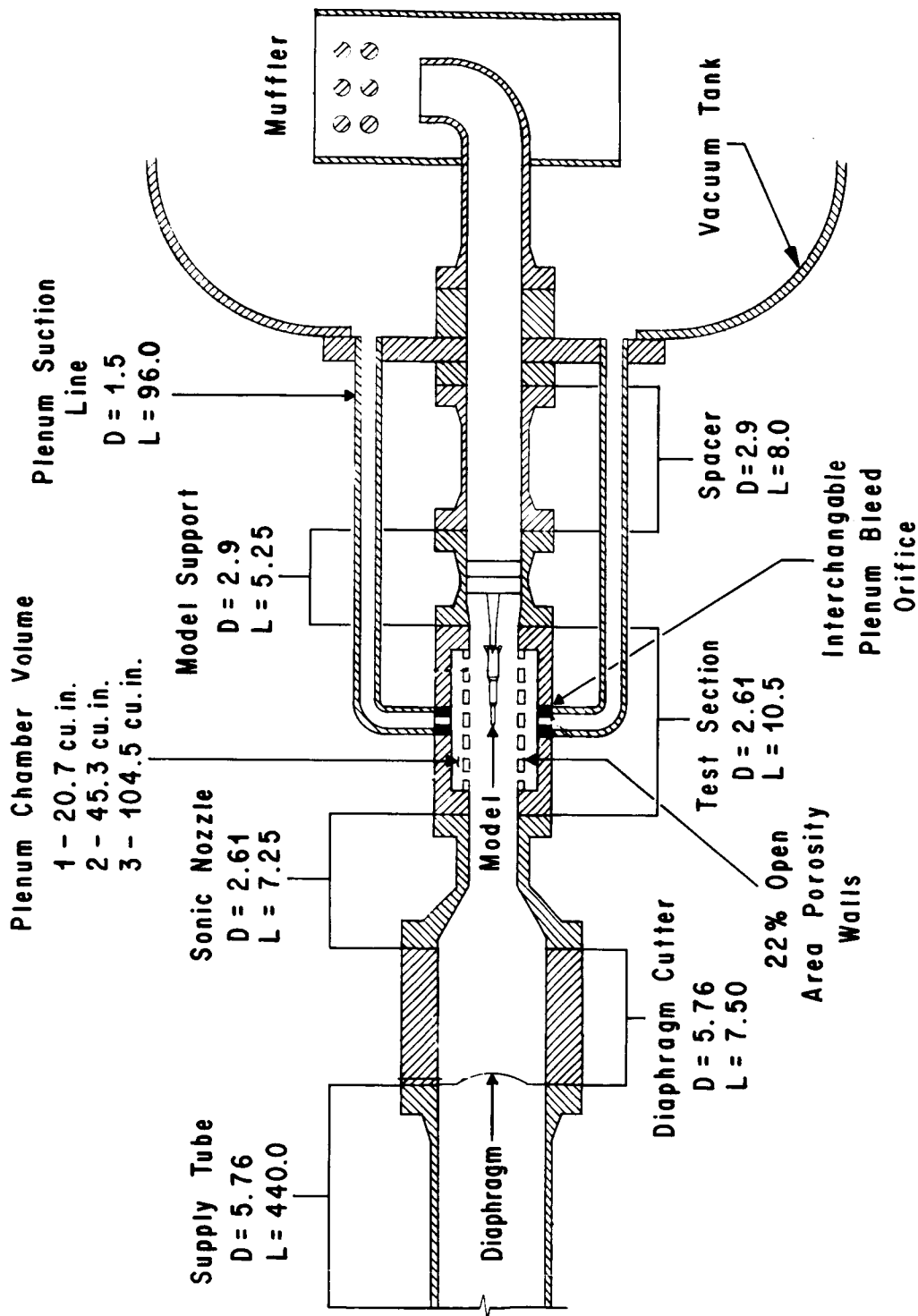
FIG. 5C. PILOT MODEL HIGH REYNOLDS NUMBER FACILITY
TRANSONIC TEST SECTION CONFIGURATION
UPSTREAM DIAPHRAGM POSITION

23

Strain Gage

0.261"

2.448"
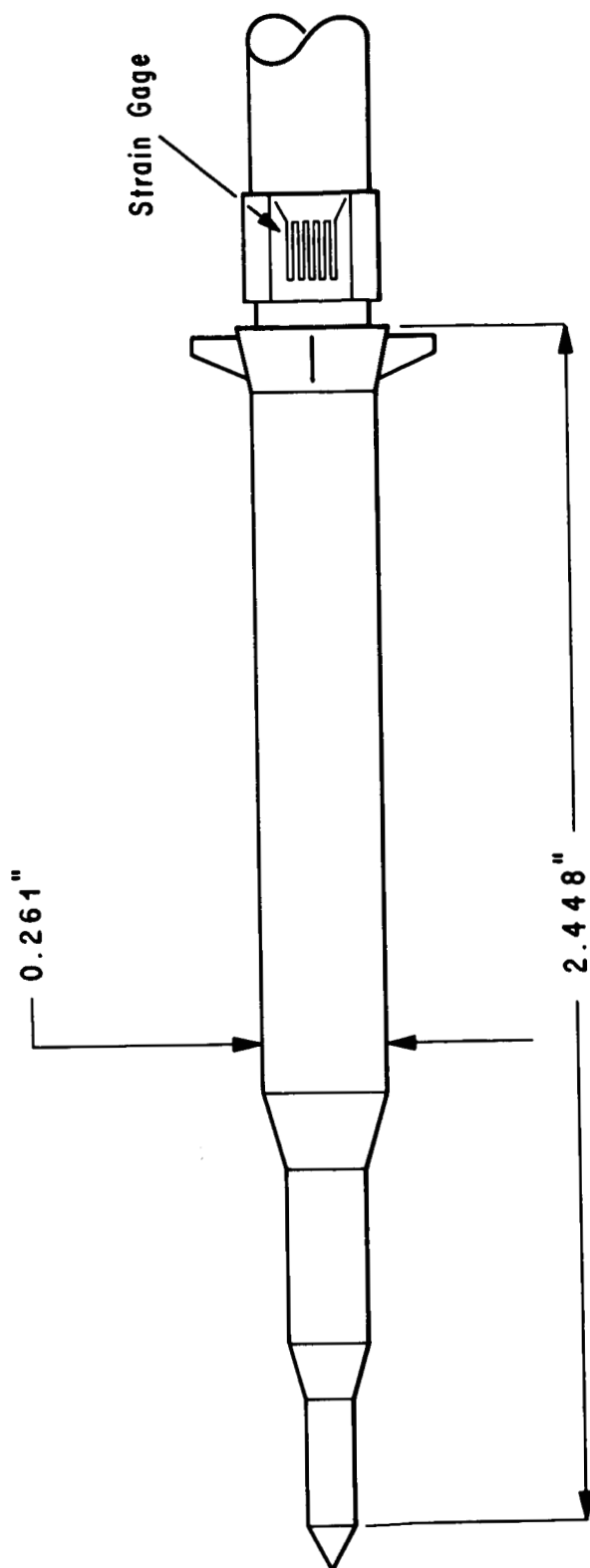
FIG. 6. STARTING LOAD MODEL CONFIGURATION
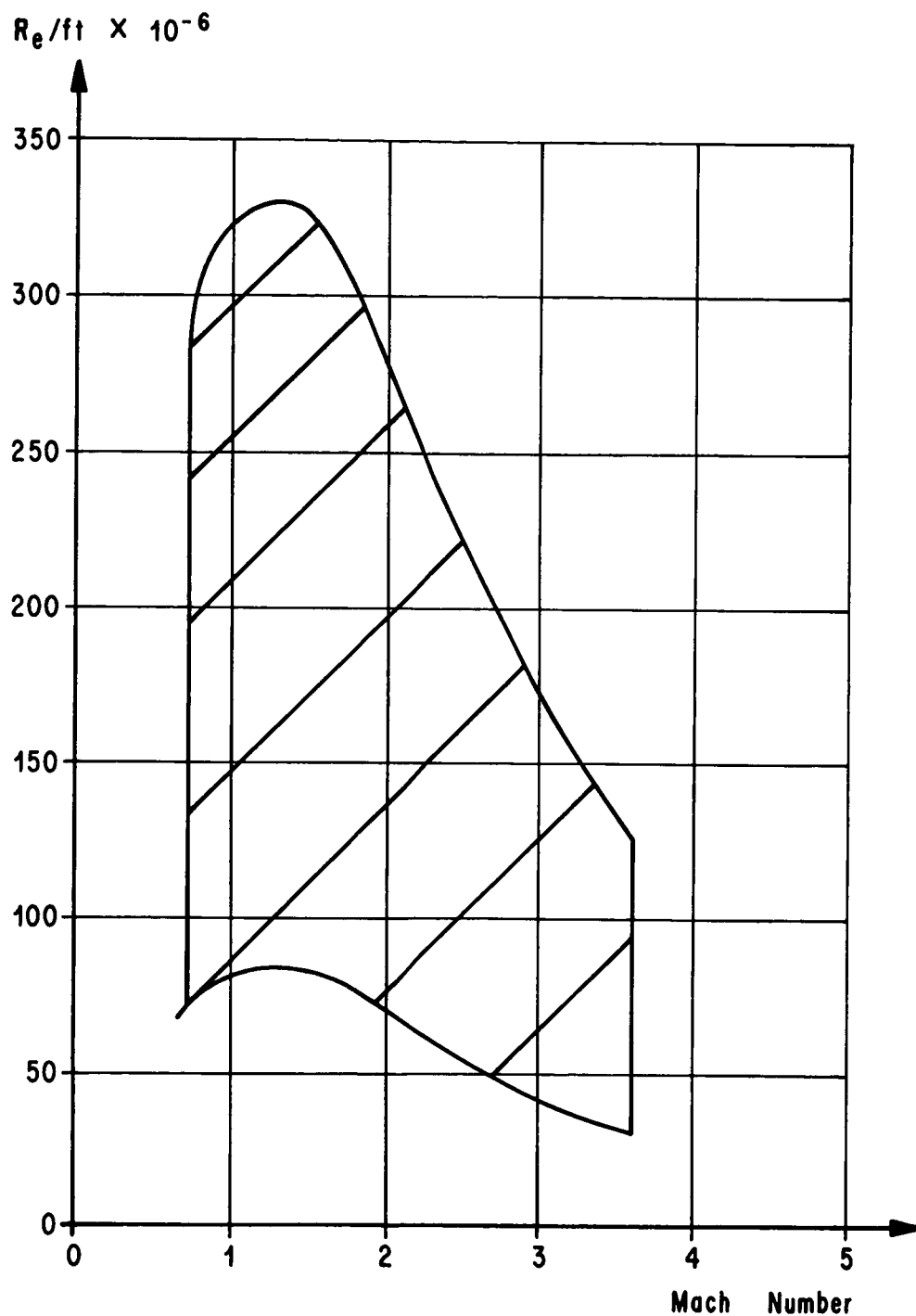
FIG. 7. TEST REYNOLDS NUMBER RANGE
AS A FUNCTION OF MACH NUMBER
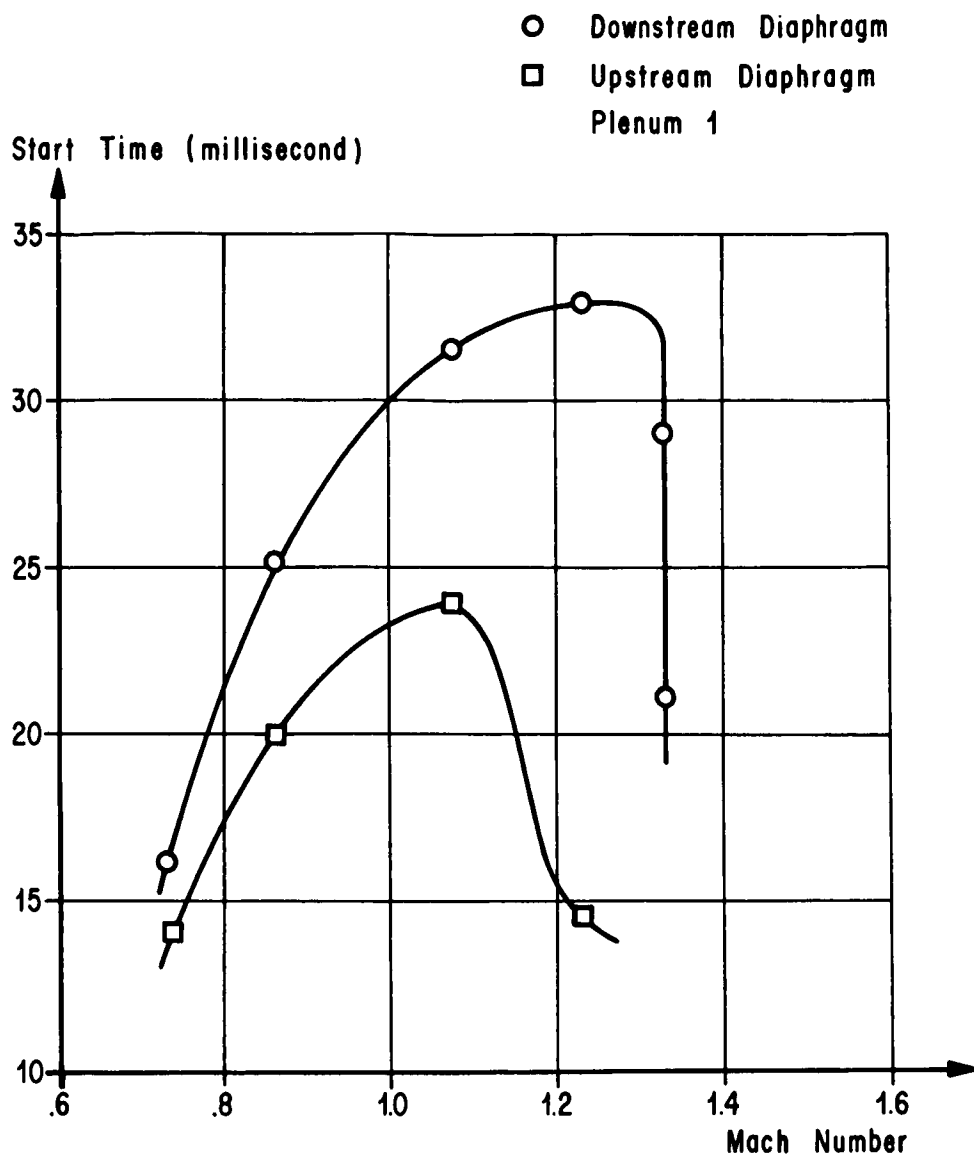
FIG. 8A. TRANSONIC TEST SECTION STARTING CHARACTERISTICS
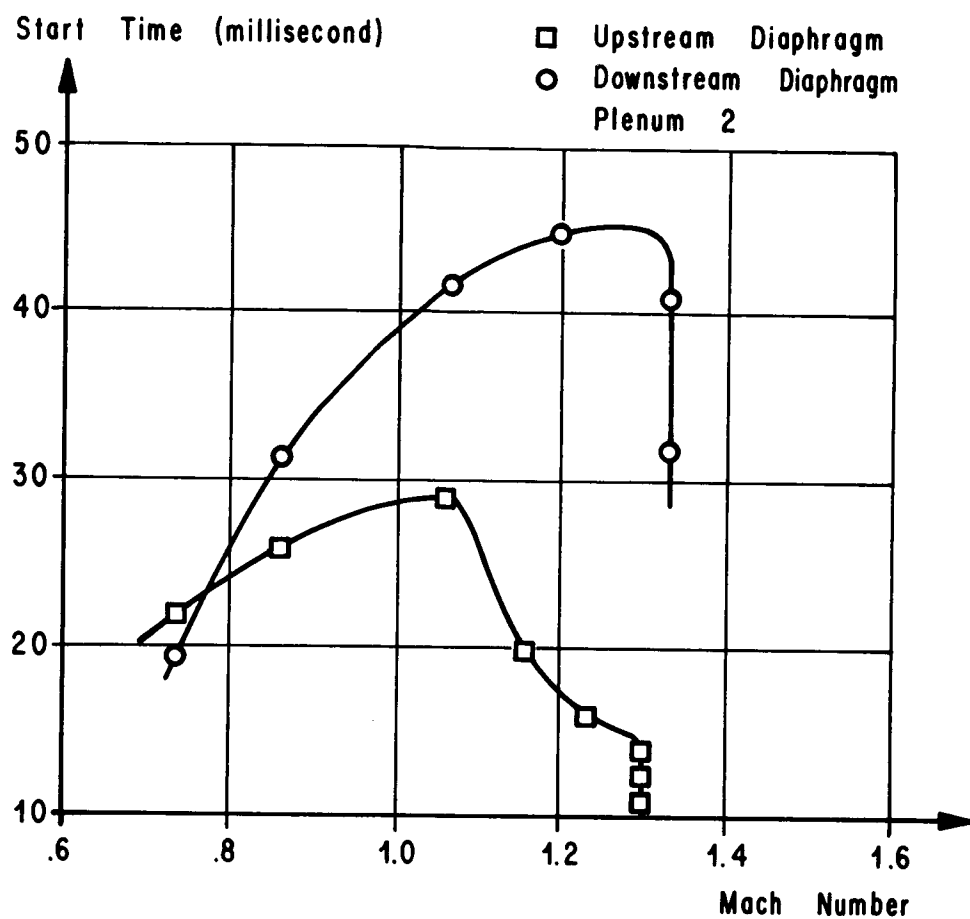
FIG. 8B. TRANSONIC TEST SECTION

STARTING CHARACTERISTICS
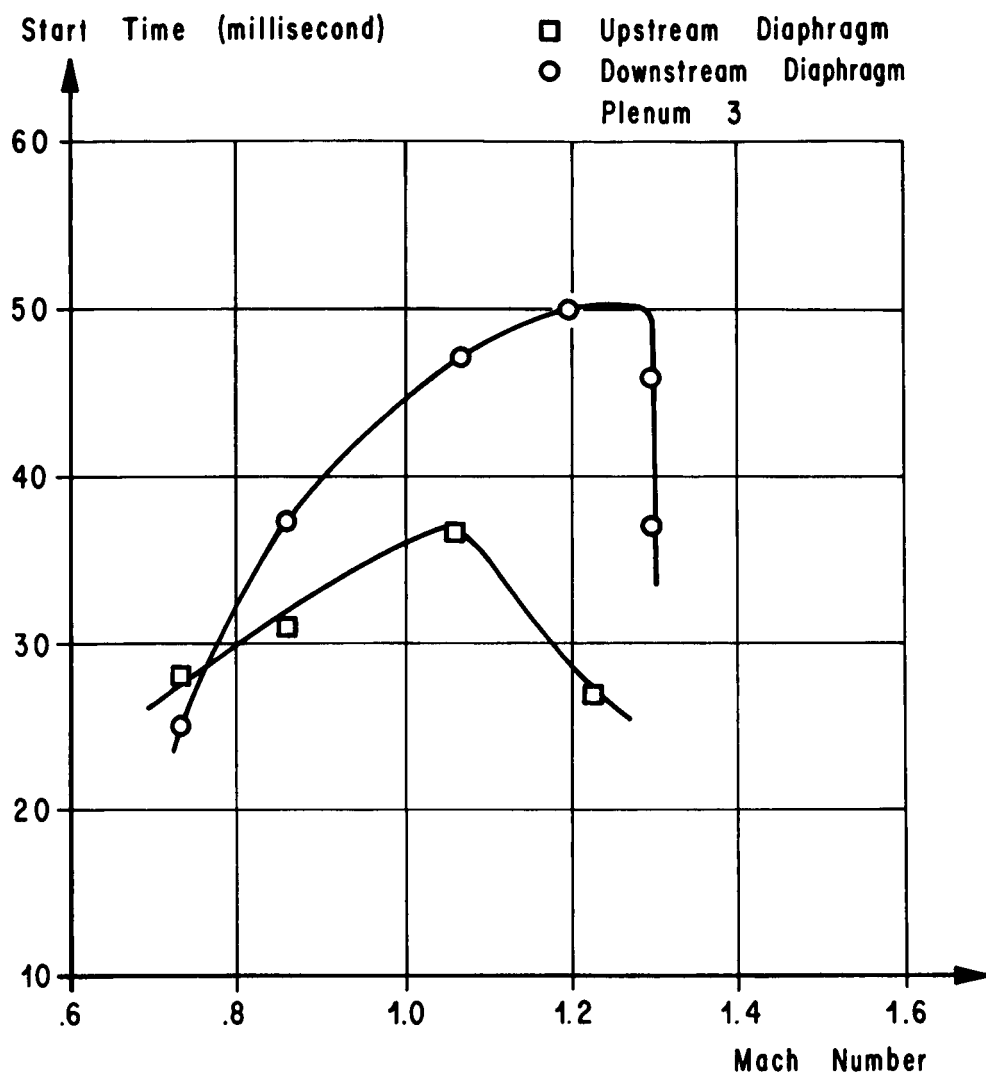
FIG. 8C. TRANSONIC TEST SECTION
STARTING CHARACTERISTICS
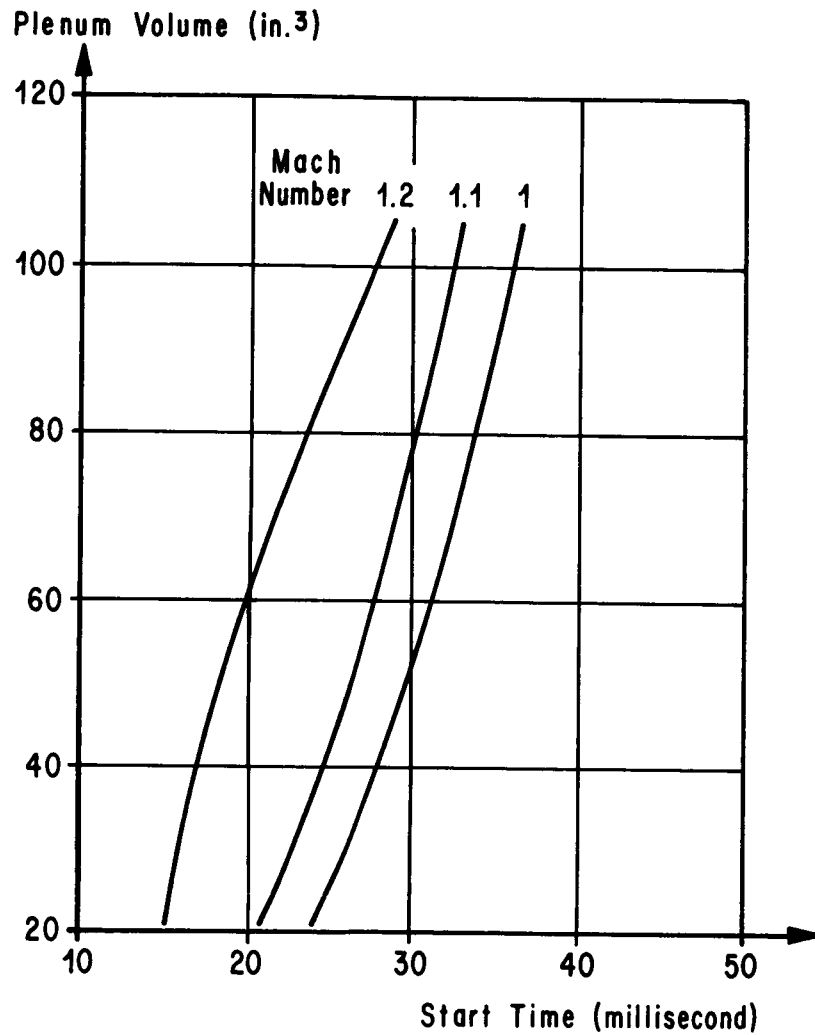
FIG. 9A. TRANSONIC START TIME IN RELATION TO
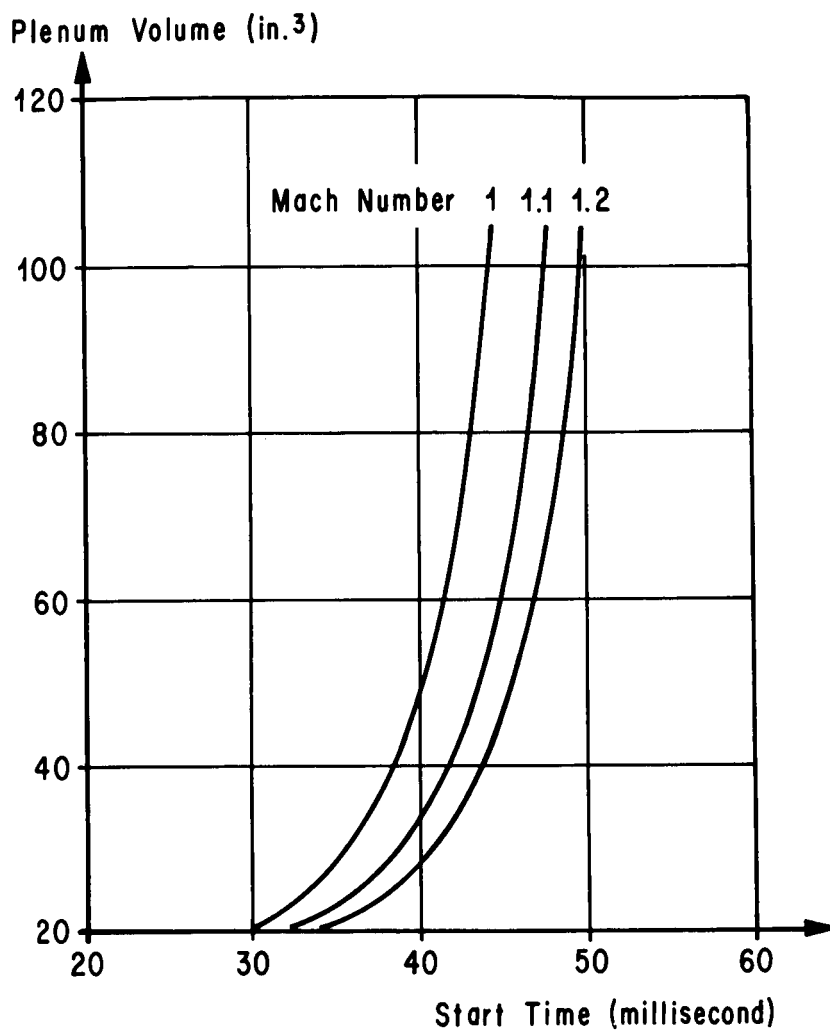PLENUM VOLUME FOR AN UPSTREAM DIAPHRAGM

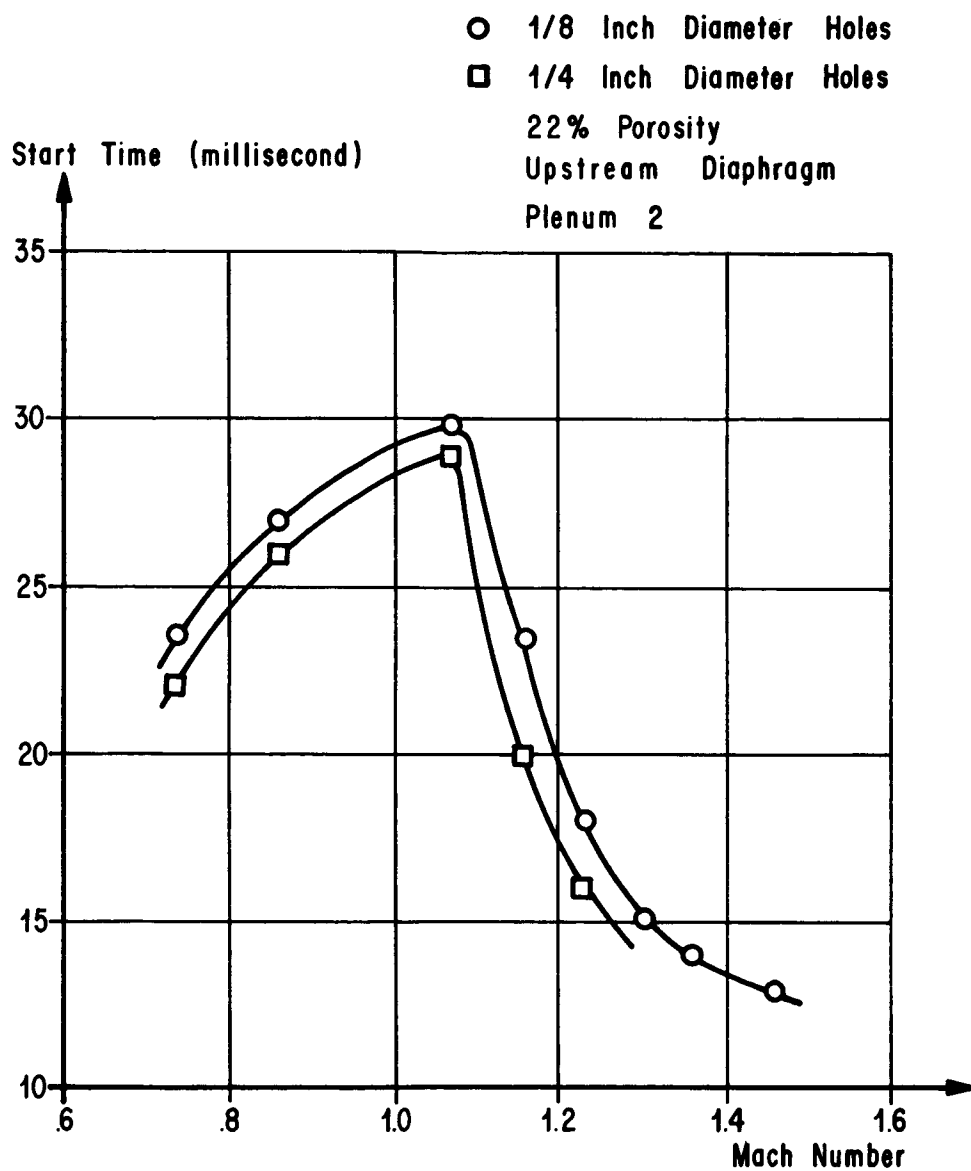FIG. 9B. TRANSONIC START TIME IN RELATION TO
PLENUM VOLUME FOR A DOWNSTREAM DIAPHRAGM

FIG. 10A. EFFECT OF TEST SECTION HOLE SIZE
ON START TIME FOR CONSTANT POROSITY WALLS
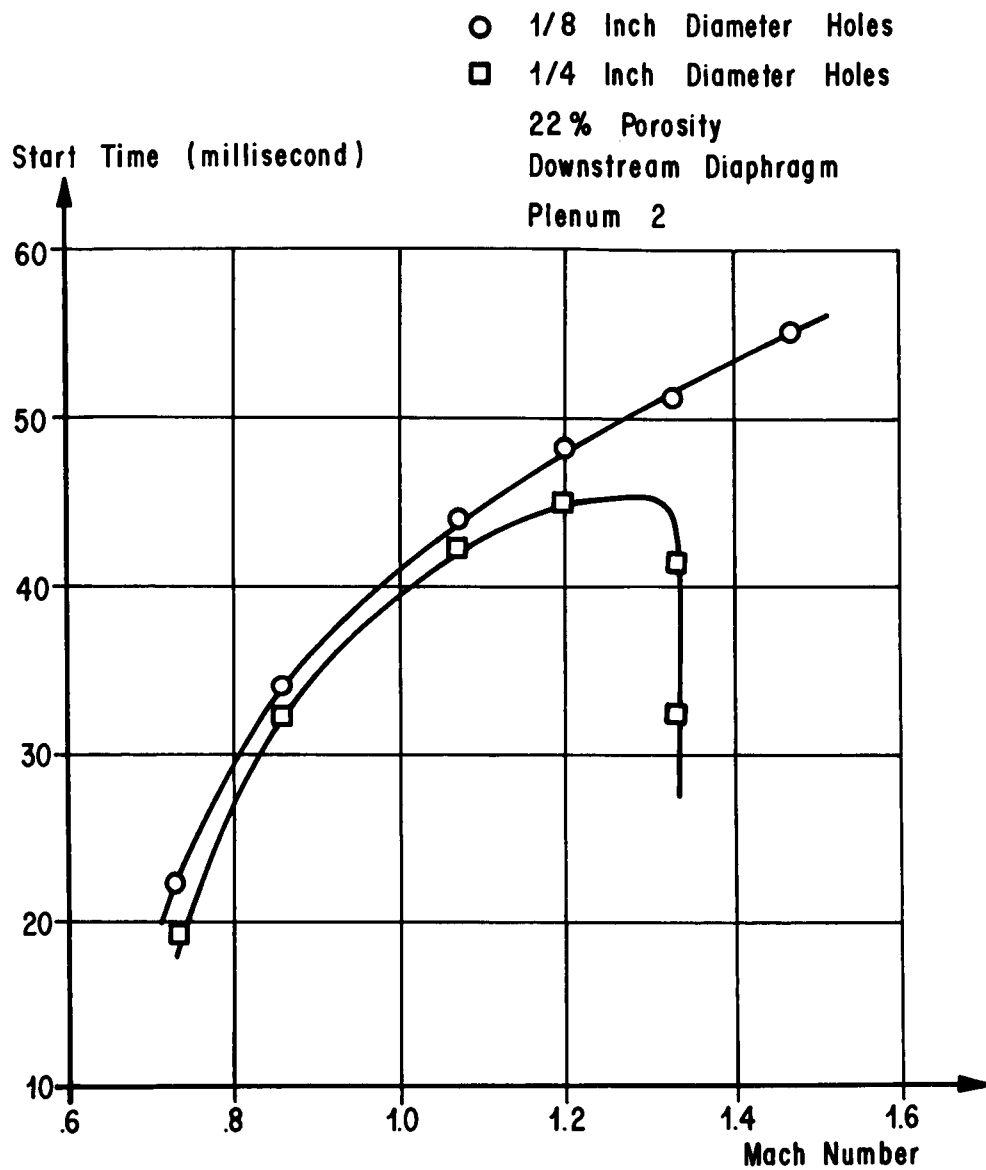
FIG. 10B. EFFECT OF TEST SECTION HOLE SIZE
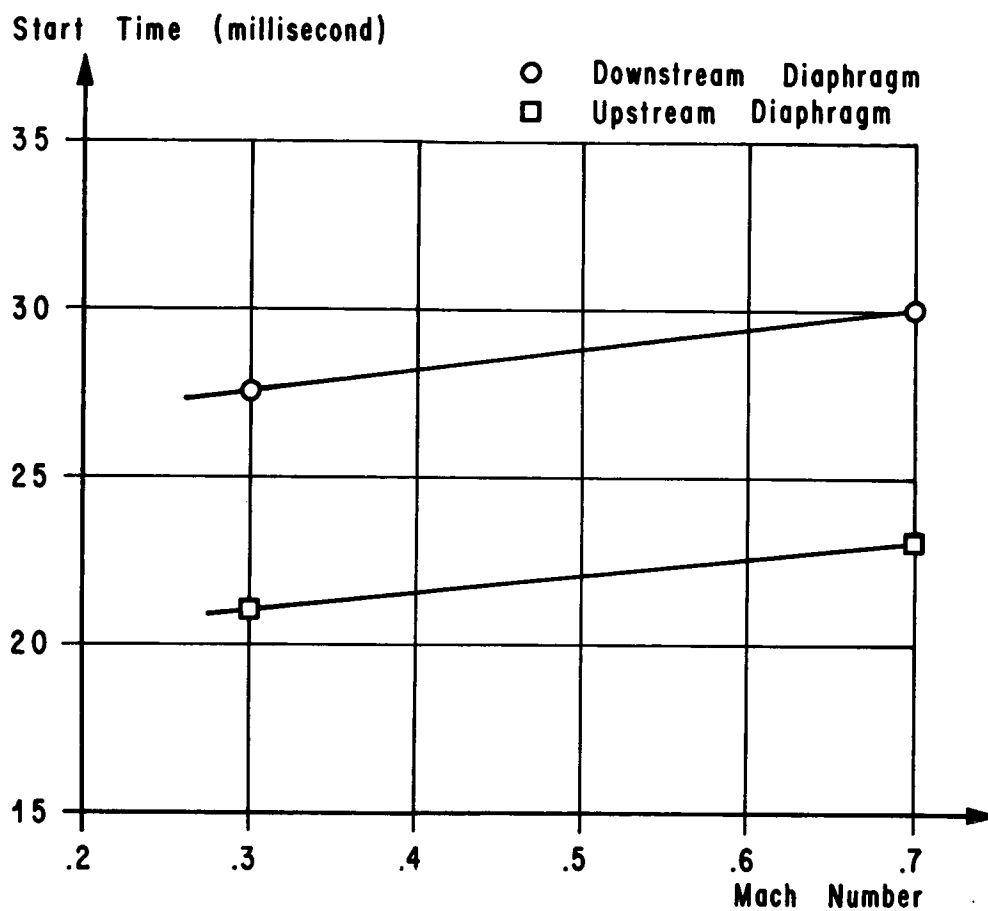ON START TIME FOR CONSTANT POROSITY WALLS

FIG. 11A. SUBSONIC AND SUPERSONIC TEST SECTION
START TIME COMPARISONS FOR
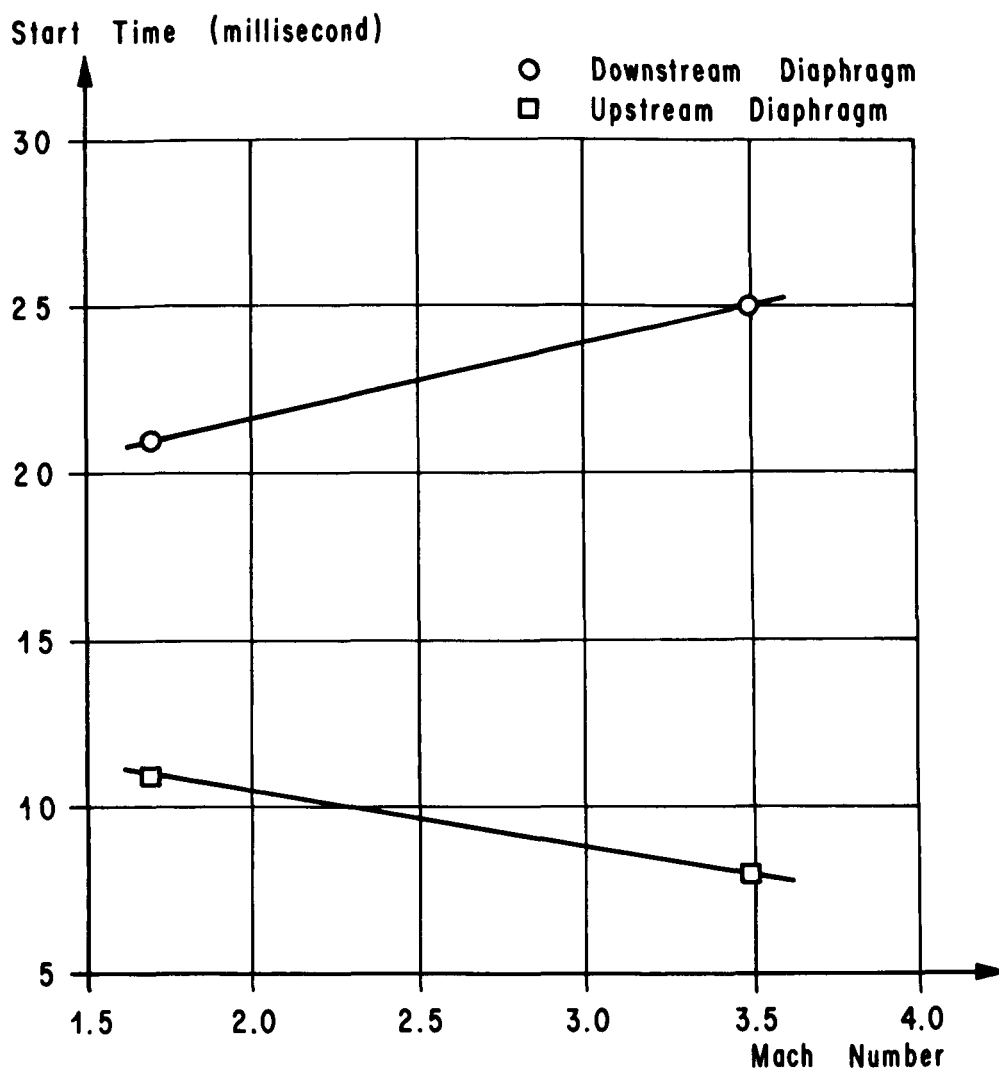UPSTREAM AND DOWNSTREAM DIAPHRAGM LOCATIONS

FIG. 11B. SUBSONIC AND SUPERSONIC TEST SECTION
START TIME COMPARISONS FOR
UPSTREAM AND DOWNSTREAM DIAPHRAGM LOCATIONS

34

◇ Upstream Diaphragm With Settling Chamber
○ Downstream Diaphragm With Settling Chamber
△ Downstream Diaphragm Without Settling Chamber
□ Upstream Diaphragm Without Settling Chamber
Plenum 1

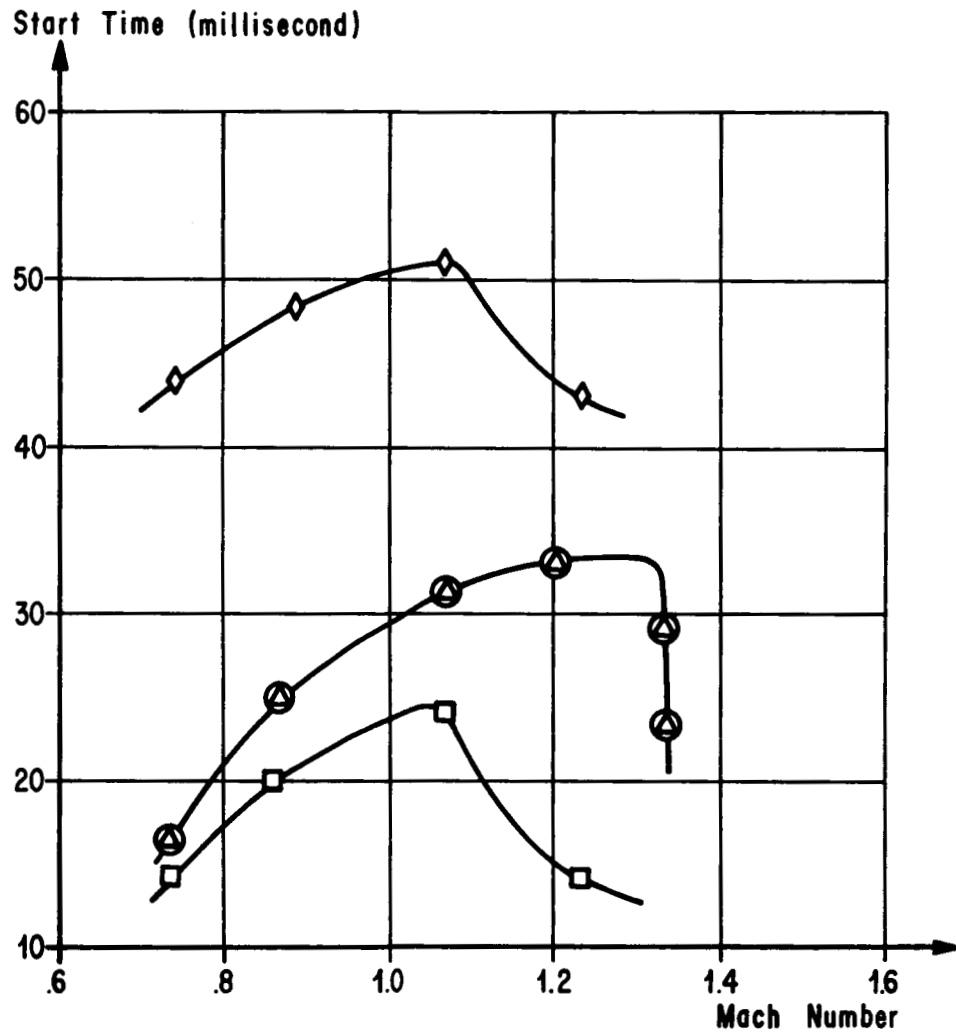Start Time (millisecond)

FIG. 12. EFFECT OF SETTLING CHAMBER
ON TRANSONIC TEST SECTION STARTING CHARACTERISTICS
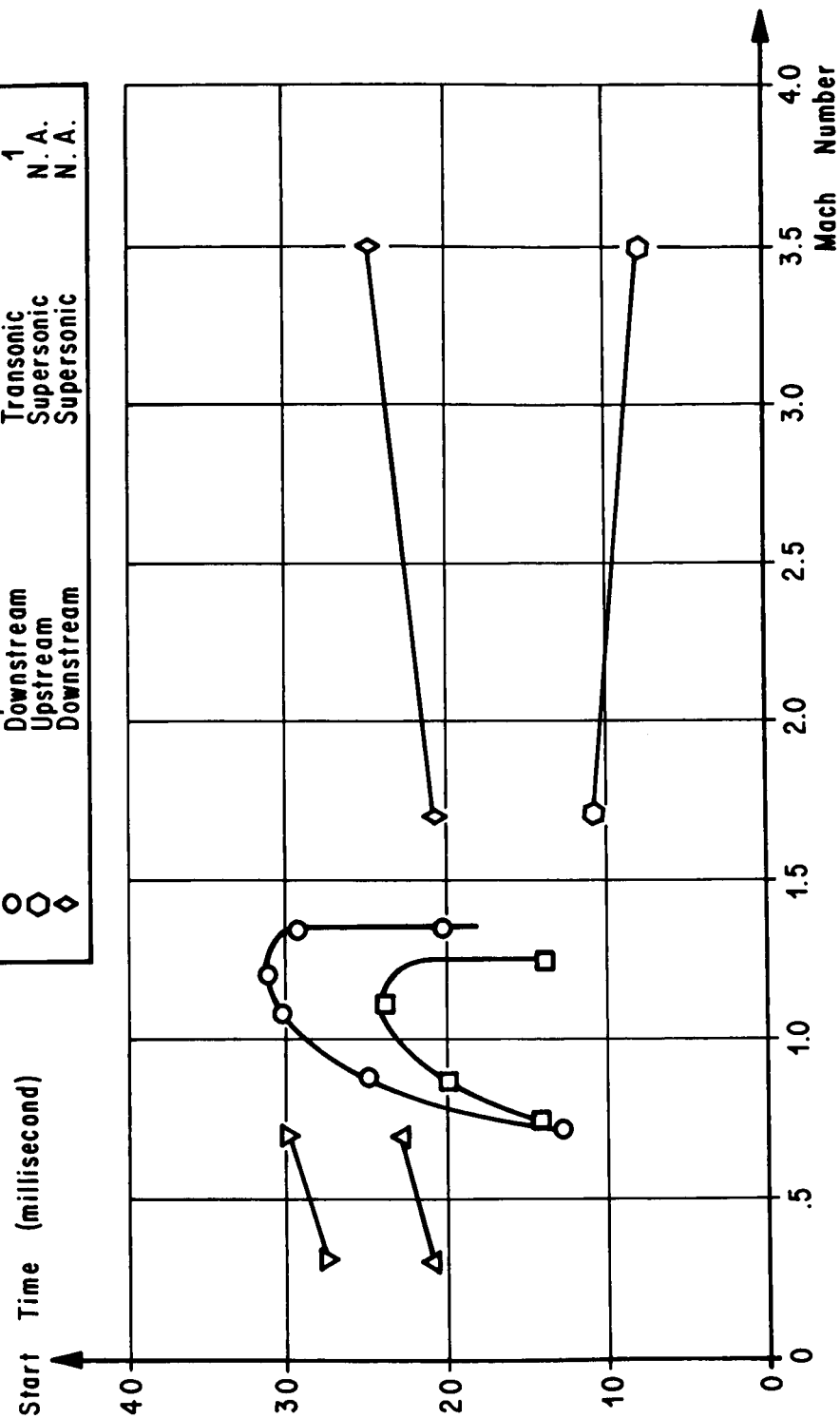
FIG. 13. TUNNEL START TIME CHARACTERISTICS
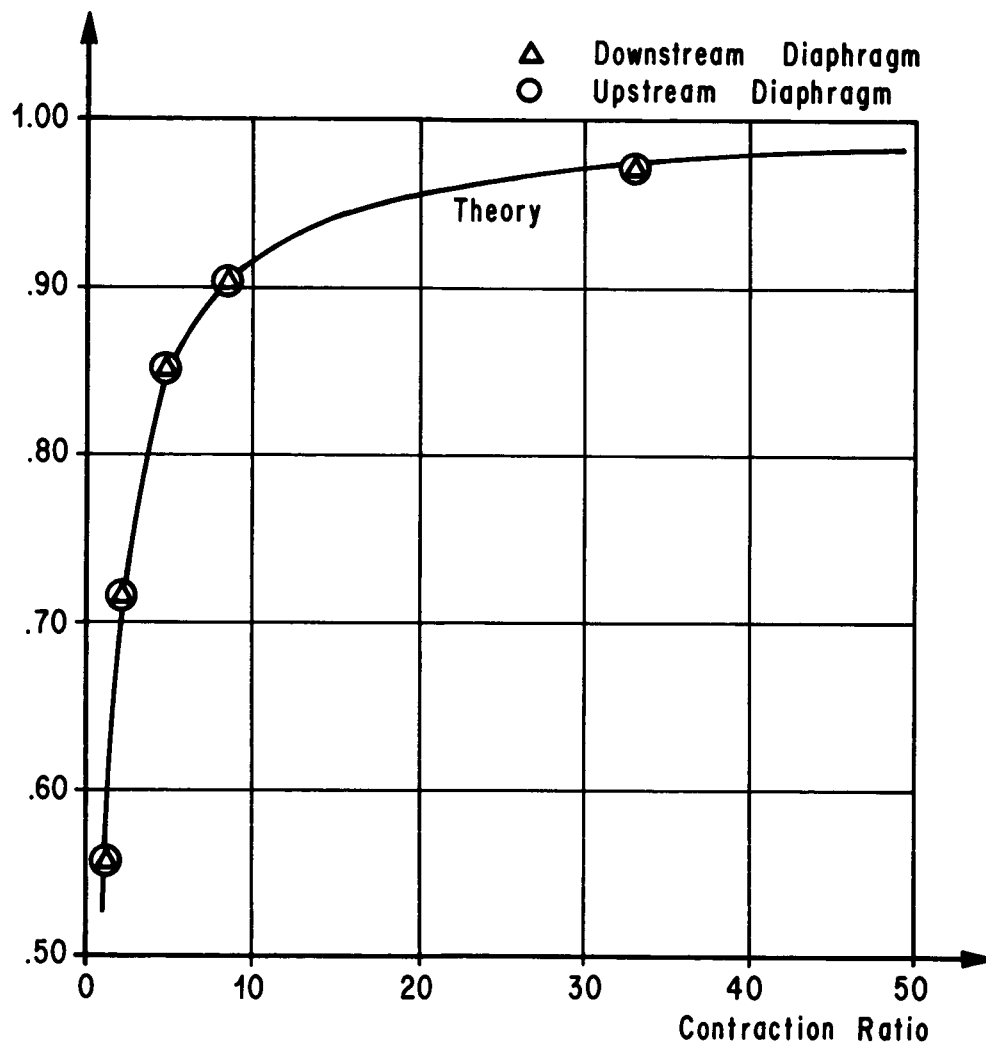OVER RANGE OF MACH NUMBERS SURVEYED

FIG. 14. COMPARSION OF THEORETICAL AND EXPERIMENTAL
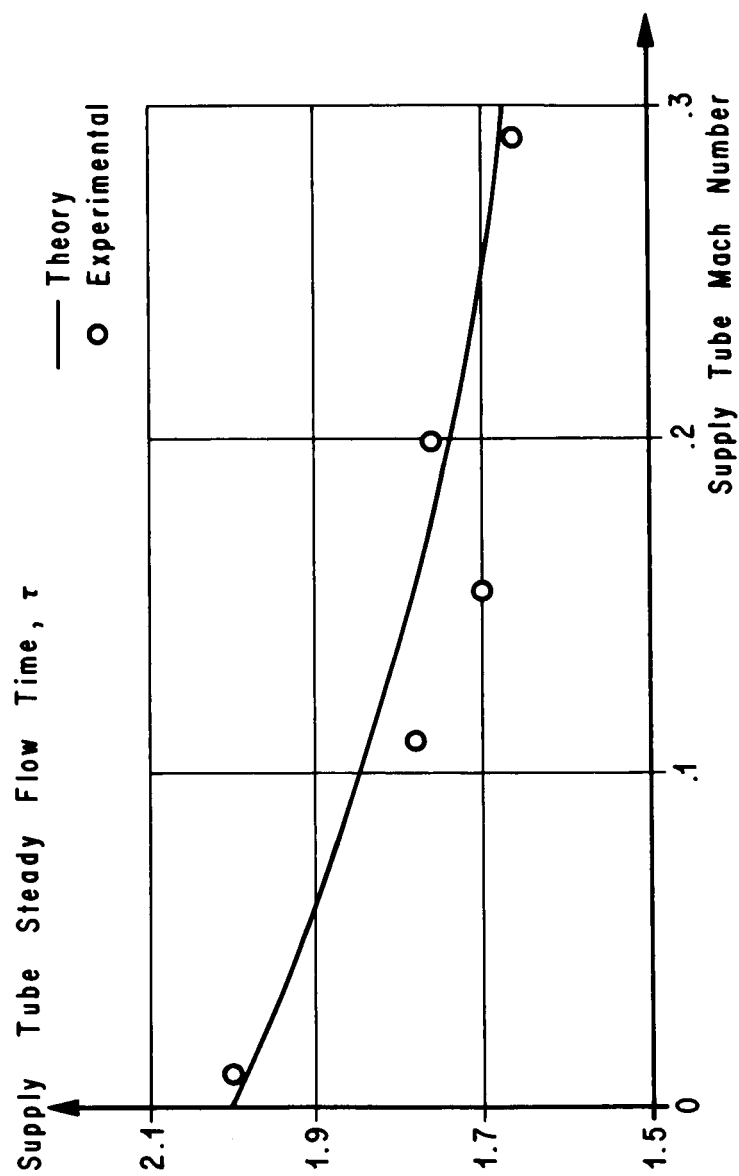RECOVERY PRESSURE IN SUPPLY TUBE

37

FIG. 15. RELATIONSHIP BETWEEN THEORETICAL AND EXPERIMENTAL
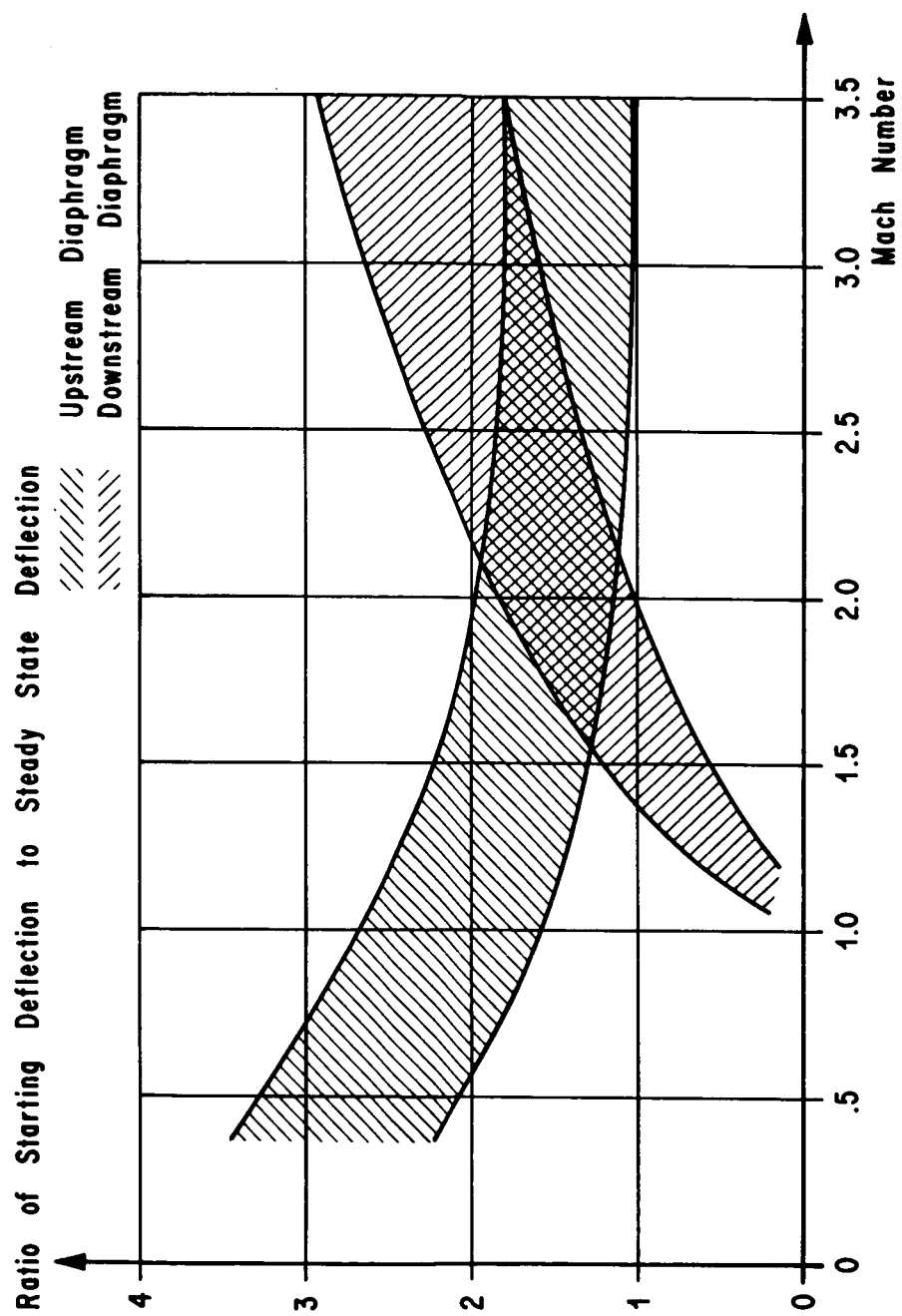STEADY FLOW TIMES IN SUPPLY TUBE FOR AN UPSTREAM DIAPHRAGM

FIG. 16. MODEL STARTING LOAD TRENDS

APPENDIX

It is desired to determine in closed form the path of the head of the incident rarefaction wave after reflecting off the closed end of the supply tube, the position at which the reflected head of the incident wave overtakes the tail of the incident wave, and finally the period in which steady flow exists in the supply tube at the nozzle entrance. These parameters can be determined by the method of characteristics. It will be convenient to transfer subsequent discussion to the nondimensional (X, τ) plane as shown below:
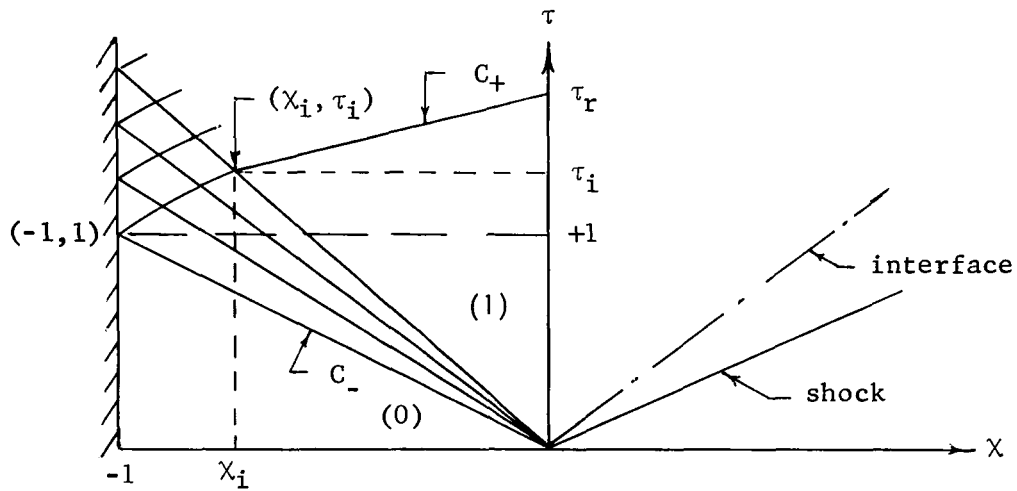
The direction of a C_- characteristic in the (X, τ) plane is for a centered wave given by

$$\frac{X}{\tau} = U - A, \tag{A-1}$$

where U and A are local dimensionless values of the particle and acoustic speeds. Further,

$$U + \frac{2A}{\gamma - 1} = U_o + \frac{2}{\gamma - 1}. \tag{A-2}$$

Since the gas in the supply tube is initially at rest, U_0 is zero, and equation (A-2) becomes

$$A = 1 - \frac{\gamma - 1}{2} U. \tag{A-3}$$

Combining equations (A-1) and (A-3) results in

$$U = \left[\frac{X}{\tau} + 1 \right] \frac{2}{\gamma + 1} \tag{A-4}$$

and

$$A = \frac{2}{\gamma + 1} - \left[\frac{\gamma - 1}{\gamma + 1} \right] \frac{X}{\tau} . \tag{A-5}$$

To determine the equation of the path of the reflected head of the incident wave through the point $(-1, 1)$ in the (X, τ) plane until it reaches the tail of the incident wave, we must solve the equation of motion for the first reflected C_+ characteristic where U and A are given by equations (A-4) and (A-5). In this interval, nonlinear interaction of the C_+ and C_- characteristics occurs. Then, for the first reflected characteristic,

$$\frac{dX}{d\tau} = U + A. \tag{A-6}$$

Equation (A-6) when combined with equations (A-4) and (A-5) becomes

$$\frac{dX}{d\tau} = \frac{4}{\gamma + 1} - \left[\frac{\gamma - 3}{\gamma + 1} \right] \frac{X}{\tau} , \tag{A-7}$$

and it follows that

$$\frac{dX}{d\tau} + \left[\frac{\gamma - 3}{\gamma + 1} \right] \frac{X}{\tau} = \frac{4}{\gamma + 1} . \tag{A-8}$$

42

This is a first order linear differential equation and may be readily solved once the integrating factor

$$\tau^{\frac{\gamma-3}{\gamma+1}}$$

has been determined. Multiplying equation (A-8) by this integrating factor yields

$$\tau^{\frac{\gamma-3}{\gamma+1}} \frac{dX}{d\tau} + \left[\frac{\gamma-3}{\gamma+1}\right] X \tau^{(\frac{\gamma-3}{\gamma+1}-1)} = \left[\frac{4}{\gamma+1}\right] \tau^{\frac{\gamma-3}{\gamma+1}} . \qquad (A-9)$$

The left member is the derivative of $X\tau^{\frac{\gamma-3}{\gamma+1}}$ with respect to τ; thus integration of equation (A-9) results in the following solution:

$$X\tau^{\frac{\gamma-3}{\gamma+1}} = \left[\frac{4}{\gamma+1}\right] \left[\frac{1}{\frac{\gamma-3}{\gamma+1}+1}\right] \tau^{(\frac{\gamma-3}{\gamma+1}+1)} + C_1. \qquad (A-10)$$

Rearranging equation (A-10) results in the relation

$$X = \frac{2}{\gamma-1}\tau + C_1 \tau^{-\frac{\gamma-3}{\gamma+1}} , \qquad (A-11)$$

where C_1 is a constant of integration which may be evaluated from the boundary condition that $X = -1$ when $\tau = 1$. This condition yields

$$C_1 = -\frac{\gamma+1}{\gamma-1} ,$$

and equation (A-11) becomes

$$X = \frac{2}{\gamma-1}\tau - \frac{\gamma+1}{\gamma-1}\tau^{-\frac{\gamma-3}{\gamma+1}} . \qquad (A-12)$$

This solution represents the path of the first reflected characteristic and applies only between the head and the tail of the incident rarefaction wave. It is convenient to write equation (A-12) as a function of the parameter

$$\alpha = \frac{\gamma + 1}{\gamma - 1}$$

such that

$$\chi = (\alpha - 1) \; \tau - \alpha \tau^{1 - 2\alpha^{-1}}. \tag{A-13}$$

Now knowing the path of the reflected head of the incident wave, we can determine the time at and position in which it overtakes the tail of the incident wave. Along the tail of the incident wave

$$\frac{\chi}{\tau} = U_1 - A_1. \tag{A-14}$$

From equation (A-3), we see that

$$A_1 = 1 - \frac{\gamma - 1}{2} \, U_1 = \frac{a_1}{a_o} \, , \tag{A-15}$$

and, from equation (19) in the text,

$$\frac{a_1}{a_o} = (P_1/P_o)^{\frac{\gamma - 1}{2\gamma}}. \tag{A-16}$$

Combining equations (A-15) and (A-16), we find that

$$U_1 = \frac{2}{\gamma - 1} \left[1 - (P_1/P_o)^{\frac{\gamma - 1}{2\gamma}} \right]. \tag{A-17}$$

44

From equations (A-15) and (A-17), we see that

$$A_1 = (P_1/P_0)^{\frac{\gamma-1}{2\gamma}} . \tag{A-18}$$

At the position where the reflected head of the incident wave overtakes the tail of the incident wave,

$$X = X_i, \qquad \tau = \tau_i,$$

and equation (A-14) becomes

$$X_i = (U_1 - A_1)\, \tau_i . \tag{A-19}$$

Therefore, by using (A-17) and (A-18), equation (A-19) takes the form

$$X_i = \left\{ \frac{2}{\gamma - 1}\left[1 - (P_1/P_0)^{\frac{\gamma-1}{2\gamma}} \right] - (P_1/P_0)^{\frac{\gamma-1}{2\gamma}} \right\} \tau_i$$

$$X_i = \left[\frac{2}{\gamma - 1} - \frac{\gamma + 1}{\gamma - 1} (P_1/P_0)^{\frac{\gamma-1}{2\gamma}} \right] \tau_i \tag{A-20}$$

$$X_i = \left[\alpha - 1 - \alpha\, (P_1/P_0)^{\beta} \right] \tau_i ,$$

where

$$\beta = \frac{\gamma - 1}{2\gamma} .$$

Also, from equation (A-13),

$$X_i = \left[\alpha - 1 - \alpha \tau_i^{-2\alpha^{-1}} \right] \tau_i . \tag{A-21}$$

45

Thus, equations (A-20) and (A-21) may be solved for the location of the point of intersection (X_i, τ_i). Then combining these relations, we obtain

$$\tau_i = (P_1/P_o)^{-\beta\alpha/2}, \tag{A-22}$$

and it follows that

$$X_i = \left[\alpha - 1 - \alpha \, (P_1/P_o)^\beta\right] (P_1/P_o)^{-\beta\alpha/2}. \tag{A-23}$$

Since the position in the (X, τ) plane where the reflected head of the incident wave overtakes the tail of the incident wave is now known, we may determine the period of time τ_r required for the head of the incident rarefaction to return to its position of origin, and thus the duration of steady flow in the supply tube, as follows:

$$\tau_r = \tau_i + [\tau_r - \tau_i]. \tag{A-24}$$

The quantity $(\tau_r - \tau_i)$ can be determined from equation (A-6) since the remaining path of the C_+ characteristic is a straight line, and U_1, A_1, and X_i are defined by equations (A-17), (A-18), and (A-23). Thus,

$$\tau_r = \tau_i - \frac{X_i}{U_1 + A_1}. \tag{A-25}$$

Substituting equations (A-17), (A-18), and (A-22) into equation (A-25) yields

$$\tau_r = (P_1/P_o)^{-\beta\alpha/2} - \frac{[\alpha - 1 - \alpha \, (P_1/P_o)^\beta] \, (P_1/P_o)^{-\beta\alpha/2}}{\dfrac{M_1}{1 + \dfrac{\gamma - 1}{2} M_1} + \dfrac{1}{1 + \dfrac{\gamma - 1}{2} M_1}}. \tag{A-26}$$

46

If we define the quantity $D = 1 + \dfrac{\gamma - 1}{2} M_1$, and substitute into equation (A-26) the value of P_1/P_0 obtained from equation (20), we obtain the following result:

$$\tau_r = D^{\alpha/2} - \frac{D^{\alpha/2}\,(\alpha - 1 - \alpha D^{-1})D}{1 + M_1} \, . \tag{A-27}$$

After simplification, it may be shown that this relation becomes

$$\tau_r = \frac{2}{1 + M_1}\left[1 + \frac{\gamma - 1}{2} M_1\right]^{\frac{\gamma+1}{2(\gamma-1)}} , \tag{A-28}$$

which is the period of time desired.

REFERENCES

1. Dahm, W. K., "Discussion of a Proposed High Reynolds Number Simulation Facility," September 10, 1965, MSFC, AERO Internal Note No. 21-65, Unclassified.

2. Ludweig, H., "Tube Wind Tunnel - A Special Type of Blowdown Tunnel," July 1957, North Atlantic Treaty Organization Advisory Group for Aeronautical Research and Development, Report 143, Unclassified.

3. Glass, I. I. and J. G. Hall, "Handbook of Supersonic Aerodynamics," Section 18, "Shock Tubes," NVORD Report 1488 (Vol. 6), December 1959, Unclassified.

4. Lukasiewiez, J., "Shock Tube Theory and Applications," National Aeronautical Establishment, Canada, 1952, Report 15, Unclassified.

5. "Equations, Tables, and Charts for Compressible Flow," National Advisory Committee for Aeronautics, Report 1135, 1953, Unclassified.

6. Bull, G. V., "Starting Processes in an Intermittent Supersonic Wind Tunnel," The Institute of Aerophysics, University of Toronto, February 1951, UTIA Report No. 12, Unclassified.

7. Bull, G. V., "Investigation into the Operating Cycle of a Two Dimensional Supersonic Wind Tunnel," The Institute of Aerophysics, University of Toronto, Jaunary 1952, Unclassified.

FEASIBILITY STUDIES OF A SHORT DURATION
HIGH REYNOLDS NUMBER TUBE WIND TUNNEL

by John W. Davis and Hal S. Gwin

The information in this report has been reviewed for security classification. Review of any information concerning Department of Defense or Atomic Energy Commission programs has been made by the MSFC Security Classification Officer. This report, in its entirety, has been determined to be unclassified.

This document has also been reviewed and approved for technical accuracy.

A. R. Felix
Chief, Experimental Aerophysics Branch

Werner K. Dahm
Chief, Aerophysics Division

E. D. Geissler
Director, Aero-Astrodynamics Laboratory

DIR

DEP-T

R-DIR

MS-IP

MS-IL (8)

MS-T (6)

CC-P

I-RM-M

MS-H

R-AERO

   Dr. Geissler
   Mr. Jean
   Mr. Reed
   Mr. Murphree
   Mr. Dahm
   Mr. Holderer
   Mr. Linsley (2)
   Mr. Wilson
   Mr. Felix
   Mr. Heaman
   Mr. Struck
   Mr. Warmbrod
   Mr. Sims
   Mr. Andrews
   Mr. J. Johnson
   Mr. Blackwell
   Mr. Walker
   Mr. Ramsey
   Mr. Pitcock
   Mr. Morgan
   Mr. Dunn
   Mr. Weaver
   Mr. Davis (20)
   Mr. Donehoo
   Mr. Hensen
   Mr. Lowery
   Mr. Bacchus
   Mr. Johnston
   Mr. Wilhold
   Mr. J. Jones

Arnold Engr Dev Cen
Tullahoma, Tennessee
  ATTN: Mr. Palco
       Mr. Davis

Cornell Aeronautical Laboratory
4455 Genessee Street
P. O. Box 235
Buffalo, New York
  ATTN: Jim Martin

Princeton University
The James Forrestal Campus
Gas Dynamics Lab.
Princeton, New Jersey
  ATTN: Prof. Seymour Bogdonoff

Dr. Ronald Smelt
Vice Pres. and Chief Scientist
Lockheed Aircraft Corp.
Burbank, California

Lewis Research Center
Cleveland, Ohio
  ATTN: G. Mandel, Library Br

Ames Research Center
Moffett Field, Calif.
  ATTN: J. Lloyd Jones

Langley Research Center
Hampton, Va.
  ATTN: Aero-Physics Div, Res Ofc
      J. V. Becker

Scientific & Technical Info Facility (25)
P. O. Box 33
College Park, Maryland 20740
  ATTN: NASA Rep (S-AK/RKT)

ME Lab, Dr. Siebel

Fac & Design, Mr. Dykes